PEOPLE'S DEMOCRATIC REPUBLIC OF ALGERIA

MINISTRY OF HIGHER EDUCATION AND SCIENTIFIC RESEARCH

UNIVERSITY AMAR TELIDJI

LAGHOUAT

Sciences of matter departement

A thesis submitted to obtain the Master degree in physics
Option: Materials physics

Project topic:

Study and characterization of quenched and tempered ferromagnetic steels by magnetic BARKHAUSEN noise technique

Presented by:

Ali TEMZOUR

Jury members:

Mr. GUEDDOUH Ahmed	MCA	President	Univ of Laghouat
Mr. HALIFA Bachir	Pr	Examiner	Univ of Laghouat
Mr. NEBAIR Hocine	MAA	Supervisor	ENS of Laghouat

Academic Year: 2021-2022

Dedications

To my dear parents

To my teachers

To my family

To my friends

Thanks

This work was carried out at the LPM materials physics laboratory of the university of LAGHOUAT, in collaboration with the LGP process engineering laboratory of LAGHOUAT.

I especially thank Professor LEFKAIER Iben Khaldoun, director of the LPM laboratory and who authorized me to carry out this work in his laboratory.

I especially thank Professor HALIFA Bachir for the moral support throughout this work.

I would also like to thank Dr. MANSOURI Taher for the trust he placed in me by allowing me to benefit from his experience in metallurgy.

My thanks also go to the members of the jury, Dr. GUEDDOUH Ahmed of the University of LAGHOUAT and Mr. HALIFA Bachir of the University of LAGHOUAT, for agreeing to examine this manuscript and to be its rapporteurs as well as for their encouragement.

My thanks go to Dr. NEBAIR Hocine, who have always spared part of their time to discuss with me and guide me with his advices, I had the honor and the chance to work with him in conviviality.

I cannot finish this preamble without thanking GHEZAL Chamseddine for their continual presence and their unconditional support .

List of notations

L	$[\mathrm{m}]$	Length
D	$[\mathrm{m}]$	Seed Diameter
S_2	$[\mathrm{m}^2]$	Section
V_3	$[\mathrm{m}^3]$	Volume
N	$\mathrm{s.u}$	Number of turns
T	$[°\mathrm{C}]$	Temperature
C_1	$[°\mathrm{C}^{-1}]$	Curie constant
K_1	$[\mathrm{J.K}]$	Boltzmann constant
I	$[\mathrm{A}]$	Electric power
U	$[\mathrm{mV}]$	Potential difference
R	$[\Omega]$	Electrical resistance
σ_1	$[\mathrm{S.m}^{-1}]$	Electrical conductivity
ρ_J	$[\Omega\mathrm{m}]$	Electrical resistivity
J	$[\mathrm{A.m}^{-1}]$	Current density
E_1	$[\mathrm{V.m}^{-1}]$	Electric field
D_2	$[\mathrm{C.m}^{-1}]$	Electrical induction

List of abreviation

TTT	Temperature Time Transformation Diagram of Austenite in Isothermal Conditions
AC1	Transformation start temperature
AC3	End of transformation temperature
MS	Martensite Start temperature
Mf	Martensite Finish temperature
TRC	Continuous Cooling Transformation Diagram
Fe-C	Iron-Carbon Diagram
HLE	High Elastic Limit of steel
HSLA	Low Elastic Limit of Alloy steel
DP	Dual Phase Steels
Austé	Austenitizing Heat Treatment
DQ	Direct Quenching Heat Treatment
IQ	Intermediate Quenching Heat Treatment
SQ	Step Quenching Heat Treatment
F	Ferrite
P	Perlite
M	Martensite
B	Bainite
Cm	Cementite
MEB	Electronique scanning microscope
NITAL	Chemical etching solution (alcohol with 4% nitric acid)
HV	Hardness of Vickers
C	Centered Cubic crystal structure
BB	Bruit BARKHAUSEN
MBN	Magnetic BARKHAUSEN Noise
3MA	Micro Magnetic Microstructure and Stress Analyser
MikroMach	Mobil Micro Magnetic Analysis Characterization
SC	Slow cooling
SHT	Surface Heat Treatment

Summary

List of Figures and tables

General Introduction

In electrical engineering, the determination of the magnetic field in structures is essential in order to optimize the design of equipment from both an economic and a technical point of view. Indeed, the operation of conventional electrotechnical devices such as motors, alternators or transformers is closely linked to the distribution of the magnetic field within their structures. Knowledge of such a distribution makes it possible to calculate the quantities necessary for dimensioning such as, for example, flux, losses, etc [1].

As long as ferritic steels are ferromagnetic, BARKHAUSEN noise analysis of these steels can be used as a non-destructive evaluation technique [2]. The double sensitivity of the phenomenon to stresses, and to microstructure, gives a wide range of potential applications to the technique. Indeed, the BARKHAUSEN noise technique has already been used to assess the quality of heat treatment, to measure the depth of surface treatment, or to detect grinding burns. This explains why, over the past 20 years, the effect of crystal microstructure characteristics on BARKHAUSEN magnetic noise has been widely studied in steels, and the influence of the size of grains, precipitated carbide, ferrite, pearlite and martensite [3].

The objective of this work is the measurement of the magnetic properties of some ferromagnetic materials where we are particularly interested in alloy steels used for the transport of hydrocarbons under a service pressure of 70.52 bars, including two denominations API X70 according to the specification imposed by the API 5L “American petroleum Institute” standard [4].

We present in the first chapter, presents the basics necessary for the study of magnetic materials. This study is based on more than a century of design and manufacturing theory and practice in the field of magnetic materials. The design of electrotechnical devices with conventional laminated materials, which are the most important for electrical engineering in terms of volume, and iron oxide powder (ferrites) can be described as mature: few changes have occurred over the recent years in machine, transformer and inductor topologies and the magnetic materials used to build them. The objective of this chapter is to give a classification of materials according to their magnetic properties. To do this, two studies will be presented; a microscopic study that focuses on the origin of magnetization and the other macroscopic.

In this chapter, we also focus on the BARKHAUSEN noise technique. The measurement instrument and settings, as well as the measuring string and the different information acquired.

We will present in this second chapter, the material of study, the chemical compositions, the structures and the mechanical properties of steel for grade X70.

In the third chapter, in the first part of this chapter, we present the steel studied and the heat treatment that have been carried out. A second part will then be dedicated to the presentation of the experimental techniques used to characterize this steel.

Reference

[1] O. DEBLECKER, "Contribution à la modélisation des champs magnétiques dans les systèmes comportant des milieux non linéaires et hystérétique", Thèse de Doctorat en Sciences Appliquées, Faculté Polytechnique de Mons, Belgique, Mars 2001.

[2] Cherif Salma, Modélisation électromagnétique de système multi capteurs pièces a défauts complexes pour le contrôle non destructeur Par courants de foucauldt. UNIV-Tizi-Ouzou, 2011.

[3] O. Saquet, J. Chicois, A. Vincent, BARKHAUSEN noise from plain carbon steels: Analysis of the influence of microstructure, Groupe d'Etudes de Métallurgie Physique et Physique des Matériaux (GEMPPM, UMR CNRS 5510). L'INSA de Lyon, 1999.

[4] I. Altpeter, R. Tschuncky, K. Szielasko, Électromagnétique techniques for materials characterization, Materials Characterization Using Non destructive Evaluation (NDE) Methods, Formerly Fraunhofer Institute for Nondestructive Testing (IZFP), Saarbr€ucken, Germany, 2016.

Chapter I: General information of magnetic materials

I.1 Introduction

Magnetism is defined as the property of a magnet (a body attracted iron or steel) by which a body exhibits a defined behavior against a magnetic field, and thus we will discuss this behavior in this chapter.

Because of their numerous technological applications, magnetic materials have, on a global scale, an economic importance comparable to that of semiconductors. Research undertaken in recent years and actively pursued today in laboratories in industrialized countries has enabled the synthesis of new magnetic materials with ever higher performance.

This chapter covers the fundamentals of magnetic materials research. This research is based on more than a century of magnetic materials design and manufacture. The design of electrotechnical devices with conventional laminated materials, which are the most important in terms of volume for electrical engineering, and iron oxide powder (ferrites) can be described as mature: in recent years, few changes have occurred in machine, transformer, and inductor topologies and the magnetic materials used to build them. The goal of this chapter is to classify materials based on their magnetic properties. Two studies will be given to accomplish this: one microscopic study concentrating on the genesis of magnetism and the other an experimental study.

We chose the BARKHAUSEN noise technique to measure the magnetic properties of ferromagnetic materials (materials that are strongly magnetized in the magnetizing direction when placed in an external magnetic field, such as nickel, iron, cobalt, and rare earth metals) in the presence of a variable external magnetic field $\vec{H}$. As a result, the focus of this chapter is on this strategy. This chapter depicts the measurement apparatus and settings, as well as the measuring string and the various data obtained.

I.2 Magnetism

I.2.1 The magnetic field

A magnetic field $\vec{H}$ is a region of space where a magnetic needle is subjected to a magnetic force so this field is characterized by its vector. It is composed of at least two poles, a north pole (emissive, a positive pole (+)) and a south pole (receptive, a negative pole (-)). The lines of force always start from the North Pole towards the South Pole [1].

The magnetic field is made up of "field lines," which are lines of force that traverse the permanent magnet from side to side along the axis of the poles to close outside the magnet. These are orientated in the exterior of the magnet from north to south and make closed and unbroken curves [2].

When an electrical device is in operation, i.e. when current is flowing through the power cable, there is both an electric field and an induced magnetic field. Magnetic induction is related to the passage of current (i.e., the movement of electrons) through an electric wire. The magnetic field $\vec{B}$ expresses the capacity of a magnetic object to create an effort [3].

I.2.2. Unit of measurement

In the international system (S.I.) the fundamental legal unit of measurement of the magnetic field (magnetic induction) is the Tesla (symbol T), using a set formed by the probe and the millivolt meter constitutes a tesla- meter [3].

The probe itself consists of a small parallelepiped formed of a semiconductor through which a current flows. When the probe is "immersed" in a magnetic field, there appears between two of these faces a low voltage which is measured by a millivoltmeter. The millivoltmeter is graduated directly in teslas. Another unit sometimes used is the Gauss (G), One Gauss is equivalent to 100 μT [3].

I.2.3 Magnetic permeability

The magnetic permeability μ of a material is defined as the ratio between the norm of the magnetic induction $\vec{\mathbf{B}}$ and that of the magnetic field $\vec{\mathbf{H}}$ applied to the material. It is expressed in Henry ($H.m^{-1}$). So under the effect of an external magnetic field $\vec{\mathbf{H}}$, a magnetic induction field $\vec{\mathbf{B}}$ is created in the materials [4]:

$$\vec{\mathbf{B}} = \boldsymbol{\mu_r} \times \boldsymbol{\mu_0} \times \vec{\mathbf{H}} \qquad (\mathbf{I.1})$$

With,

$\vec{\mathbf{B}}$: induction field, expressed on Tesla

$\boldsymbol{\mu_0}$: vacuum permeability ($H.m^{-1}$)

$\vec{\mathbf{H}}$: intensity of the magnetic field ($H.m^{-1}$)

To characterize the magnetic behavior of a material, the relative permeability μ_r is often used. Hence μ is the absolute permeability (H.m^{-1}) and μ_0 is the vacuum permeability (H.m^{-1})

We define [4]:

$$\boldsymbol{\mu_r = \mu \times \mu_0} \qquad (\mathbf{I.2})$$

$$\boldsymbol{\mu_0 = 4\pi \times 10^{-7}\, H.m^{-1}} \qquad (\mathbf{I.3})$$

Some usual values of relative permeability [4]:

Table I.1 - Values of relative permeability

Matter	**Relative permeability μ_r**
Soft iron	10000
Fer-Sicilium	20000
Fer-Nickel	90000

In general, diamagnetic and paramagnetic materials have relative permeability values close to 1. The absolute permeability of diamagnetic and paramagnetic materials is therefore practically equal to that of vacuum, i.e $4\pi \times 10^{-7}\ H/m$ [4].

In a similar way, in magnetism, we introduce the magnetization noted M characterizing the nature of the magnetic object [4].

Magnetic phenomena are at the origin of the interaction of charges in motion, therefore a physical effect linked to the existence of charges in motion. The magnetic field can be created by magnetic moments in a material, the existence of these magnetic moments is linked [4]:

- ✓ The movement of elementary particles: orbital magnetic moment.
- ✓ To the spin of these particles: spin magnetic moment.

For any material, isolated, the magnetic moments that compose it can take a random orientation, but actually find a stable configuration dependent on the internal energy of the material, depending on the electronic structure of the material and the external magnetic excitations [5].

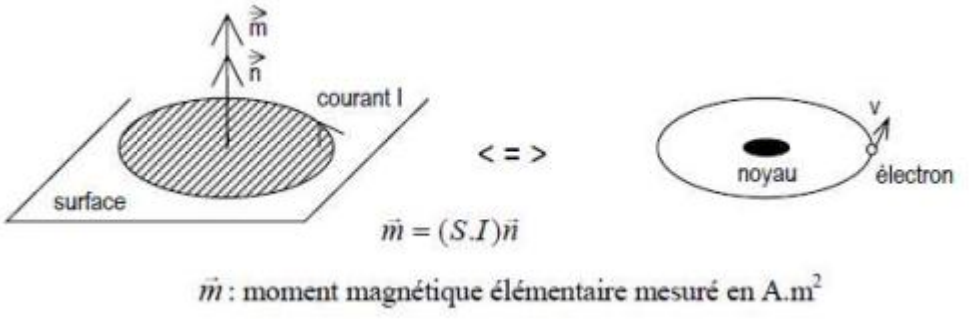

Figure I .1: Analogy electric current – particulate current [3].

Schematically, when a macroscopic system is subjected to a magnetic field, the fields $\vec{M}$ and $\vec{H}$ are linked by a relative magnetic susceptibility coefficient χ (a positive or negative dimensionless number) such that:

$$\overrightarrow{\boldsymbol{M}} = \boldsymbol{\chi}\,\overrightarrow{\boldsymbol{H}} \qquad (\mathbf{I.4})$$

This implies the following relationship:

$$\overrightarrow{\boldsymbol{B}} = \boldsymbol{\mu}_r\left(\overrightarrow{\boldsymbol{H}} + \overrightarrow{\boldsymbol{M}}\right) = \boldsymbol{\mu}_r\left(\overrightarrow{\boldsymbol{H}} + \boldsymbol{\chi}_r\,\overrightarrow{\boldsymbol{H}}\right) = \boldsymbol{\mu}_r\,\overrightarrow{\boldsymbol{H}}\,(\mathbf{1} + \boldsymbol{\chi}_r)$$

$$and\ \boldsymbol{\mu}_r = (\mathbf{1} + \boldsymbol{\chi}) \qquad (\mathbf{I.5})$$

The magnetic nature of a material is dictated by this χ value [5].

I.2.4. Main fundamental laws

- **Laplace's law**

  In a filiform circuit (C) traversed by a direct current of intensity **I** and placed in an external magnetic field $\vec{\mathbf{B}}$. An element of length $\boldsymbol{dl}$ of the circuit (C), containing dq moving charges, is subjected to a force $d\vec{F}_L$ (called Laplace force) from which [1].

  $$\boldsymbol{d\vec{F}_L = I\overrightarrow{dl} \wedge \vec{B}\ and\ \vec{v}dq = I\vec{v}dt = I\overrightarrow{dl}} \qquad (\mathbf{I.6})$$

- **Hall effect**

  Consider a flat metal strip (plate) of parallelepiped shape of length a, width b and thickness d. This ribbon is placed in a permanent and uniform $\vec{B}$ magnetic field, perpendicular to the large faces as shown in Figure (I.2) [2].

The ribbon is crossed along its thickness by a current of intensity I. The current I is due to the movement of free electrons, of speed v. In the presence of the magnetic field, these electrons are subjected to a magnetic force $\boldsymbol{d\overrightarrow{F_M}}$, normal to $\vec{v}$, which causes an accumulation of electrons on the front face of the ribbon. The accumulation of electrons on the front side and the excess of positive charges on the back side cause a potential difference between the two sides of the ribbon and an electric field $\vec{E}_H$ called the Hall field [1].

From where :

$$\boldsymbol{\vec{E}_H = \vec{V} \wedge \vec{B}} \qquad (\mathbf{I.7})$$

This field exerts on the free electrons of the volume dτ.

The steady state is reached when:

$$\boldsymbol{d\overrightarrow{F_E} = d\overrightarrow{F_M} = \vec{0}} \qquad (\mathbf{I.8})$$

The potential difference U_H called Hall voltage will be given by:

$$U_H = -\boldsymbol{I \times B \times d \times R_H} \qquad (I.9)$$

Hence:

$$R_H = \frac{1}{nq} \qquad (I.10)$$

R_H: Hall's constant (n: being the number of electrons contained in **dτ**) [1].

The value of the magnetic field B being known, the measurements of the d.d.p U_H and the intensity of the current I make it possible to determine the density of the carriers and the nature of the charges [1].

In the case where the mobile charges are electrons $R_H < 0$ and $U_H > 0$ [1].

- **Ampere's law**

  Ampère is the first to think and to demonstrate that the magnetic field is created by the electric current and not the reverse. Ampère's theorem allows us to calculate the magnetic field created by a distribution of currents, it is written under its discrete form [2]:

$$\boldsymbol{\sum B\ell = \mu_0 \sum I} \qquad (I.11)$$

integral form $\boldsymbol{\oint \vec{B}.\overrightarrow{d\ell} = \mu_0 \iint \vec{j}.\vec{n}.dS}$ (I.12)

Hence:

I: total intensity

$\vec{B}$: vector magnetic field

$\vec{j}$: vector volume distribution of the current

$\vec{n}$: vector normal to the considered surface

dS: area element

$d\ell$: element of length

The magnetic flux **Φ** is the set of field lines produced by a magnet or an electromagnet., is expressed in webers [Wb] [2].

At the macroscopic level it is interesting to express the flux of the induction vector produced by the excitation field [2] .

$$\Phi = \int \vec{B}.d\vec{S} \qquad (\mathbf{I.13})$$

- ✓ If two parallel conductors traversed by a current in the same direction, forces are exerted which tend to bring the conductors closer together.
- ✓ If two parallel conductors traversed by a current of opposite direction exert forces which tend to move the conductors away [6].

I.3. Magnetic materials

I.3.1 History of materials

Researchers are continually discovering new materials, with a prodigious variety of atomic arrangements and magnetic moments. Table (1.1) presents a historical reminder of the appearance of materials [7].

Table I.2 - history on magnetic materials

Years	**History of materials**
1880	Carbon steel, magnet (horseshoe)
1903	Fe-Si alloy (Germany, USA)
1912	Industrial production of non-grain-oriented Fe-Si
1941-1932	Grain-oriented Fe-Si sheet (Gauss 1935). Al-Ni-Co permanent magnets
1946	Ferrite magnets
1969	Rare Earth/Cobalt based magnet.

1975 -1970	Amorphous alloy, Fe-B-Si. Metallic glass.
1983	Rare earth magnets + Iron (Nd-Fe-B and Sm-Co)
1990	Premium quality mono ferrite materials

I.3.2 Definition and origin of Magnetic materials

A magnetic material appears as a set of elementary magnetic moments (atoms) interacting with each other and organized in a crystal lattice. The magnetic moments depend on the magnetic environment of each atom, namely the nature and position of neighboring atoms, the temperature and the applied magnetic field. According to the behavior of this set, we distinguish different types of magnetism: Ferromagnetism, Antiferromagnetism, Ferrimagnetism [8].

1.3.3 Different classes of materials

We are going to briefly describe the main types of magnetic behavior that can be encountered in matter [8]:

- ✓ Elements with incomplete electronic inner shells, ferromagnetic materials, ferrimagnetic and antiferromagnetic materials and paramagnetics.
- ✓ Elements with internal electronic layers complete these so-called diamagnetic materials.

1.3.3.1 Diamagnetics

We call diamagnetic the substances which present a magnetization M proportional to the field H in which they are placed and of opposite direction to this one. As shown in figure (I.3). The susceptibility of these bodies is negative and weak, of the order of 10^{-6}, i.e. the substance becomes magnetized in the opposite direction to the magnetizing field.
Example of susceptibility of Water -0.72×10^{-6} and Bismuth -1.40×10^{-6} [8].

Diamagnetic bodies include gases, solids, liquids, metalloids (other than Oxygen), metals (Gold, Silver, Mercury, Copper and Lead), salts and almost all organic substances (Benzene , Naphthalene, etc.) [8].

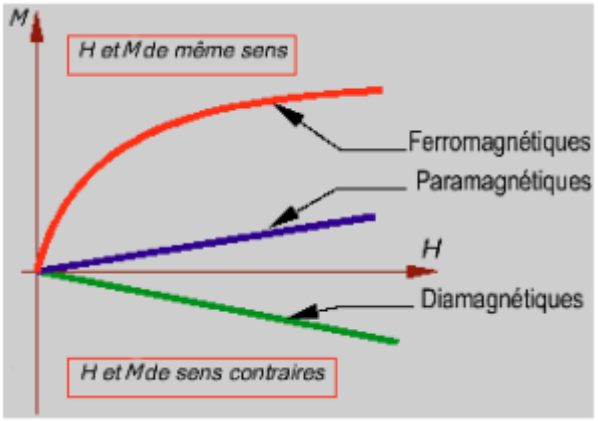

Figure I.3 : Magnetic classification of materials [8]

1.3.3.2 Paramagnetics

Substances which have a magnetization M proportional to the field H in which they are placed and in the same direction as it are called paramagnetic. For these substances, χ is positive and weak and of the order of (10^{-6}) figure (I.3) [8].

Example of susceptibility of Air $\chi = +3.8 \times 10^{-7}$ and of Oxygen $\chi = +2.0\times 10^{-5}$.

Paramagnetic substances include nitric acid, ozone and a large number of metals (Platinum, Palladium, Potassium, etc.) as well as elements from the rare earth family [8].

1.3.3.3 Ferromagnetics

Ferromagnets are substances capable of acquiring considerable magnetization, much stronger than for diamagnetics and paramagnetics. The main ferromagnetic substances are Iron, Nickel, Cobalt, Gadolinium, their alloys and some of their compounds [8].

The Ferromagnetic substances have a high magnetization, moreover it is not totally proportional to the magnetizing field as in the case of other substances. It increases and tends towards a limit called saturation magnetization, when the field $\vec{H}$ is sufficient as illustrated in figure (I.5) [8].

The magnetization is not a function of the acting field only, but it also depends on the past of the sample, or the magnetic, mechanical and thermal treatments that the sample has undergone [7].

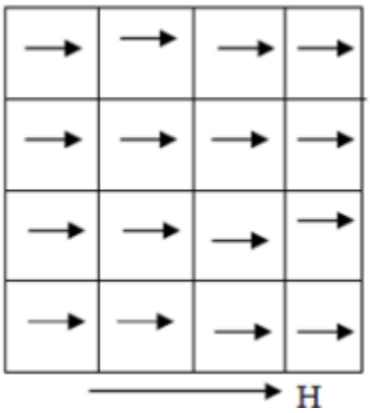

Figure 1.5 : Ferromagnetics [7]

1.3.3.4 Antiferromagnetics

For antiferromagnetics substances, the magnetic moments of the ions of the crystal lattice are oriented two by two in opposite directions; the magnetization of the whole is then zero figure (I.6). In a magnetic field, there is a slight magnetization like that of paramagnetics. The antiferromagnetics bodies include Chromium, Iron Oxide (FeO), Manganese Fluoride "MnF2" and Manganese Sulfide (MnS) [8].

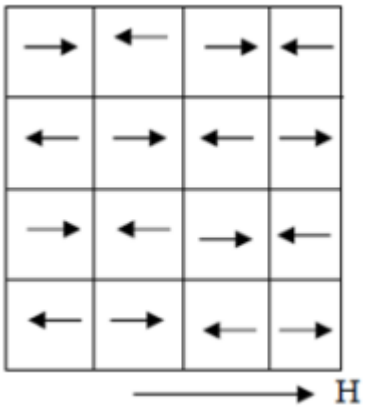

Figure I.6: Antiferromagnetism [8]

1.3.3.5 Ferrimagnetics

For ferrimagnetic substances, the magnetic moments of the crystal lattice ions are opposite and parallel, but they are unequal so the magnetic moment of the set is non-zero, as shown in figure (1.7), this is the case for compounds ferrites which are very interesting in electrical engineering,because they are practically insulating. When they are placed in a field, they are magnetized to saturation and in a spontaneous manner. The saturation magnetization is weaker than in ferromagnetic substances [8].

The general shape of these bodies X.Fe3.O4 where X represents one or more bivalent metals (Copper, Zinc, Nickel, Manganese, ….) [8].

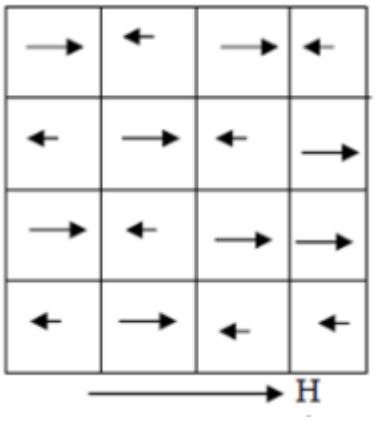

Figure I.7: Ferrimagnetism [8].

1.4. Magnetic behavior of ferromagnetic materials

1.4.1 Weiss domains

In 1907, Pierre Weiss put forward the hypothesis of magnetized magnetic domains with saturation which make it possible to measure a global moment in a zero field. The highlighting of the domains was first indirect (noise of BARKHAUZEN 1919), then direct (observation by decoration with a magnetic powder) Bitter 1931 and Harnos and Thiessen. Then the article by Landau and Lifshitz in 1935 which lays the foundations of domain theory. [9].

1.4.1.1 Exchange energy

Energy of the microscopic type, which results from the partial pooling of the trajectories of a peripheral electron between two neighboring atoms. The value of this energy is equal to the energy that would have to be provided to break this situation. It tends to align the microscopic magnetic moments of each atom [9].

1.4.1.2 The crystal anisotropy energy

In the solid state, iron, cobalt and nickel (which are the main elements of soft magnetic materials) crystallize respectively in the systems: centered cubic, hexagonal and face-centered cubic. Let us take the case of a material which would crystallize according to the centered cubic system. As we have just seen previously, the microscopic magnetic moments tend to align, due to the exchange energy that prevails between the different atoms, thus: The distance

between two neighboring atoms depends on their relative position in the lattice crystalline. The exchange energy will therefore be a function of the direction [9].

Thus, there will be directions of privileged orientations of these moments. The anisotropy energy represents the energy required to rotate all of these moments in a given direction [9].

1.4.1.3 Magnetoelastic energy

The exchange energy originates from the pooling of one (or more) electrons between two neighboring atoms and consequently the alignment of the microscopic magnetic moments of these two neighboring atoms. Thus, in a ferromagnetic sheet, due to the crystalline structure of the atoms, the distance between each atom is regular, the pooling of electrons is will always do preferentially between the physically closest atoms. Only a mechanical constraint can modify the distance separating two atoms, and thus even the pooling of . Changing the distance between atoms modifies the energy state and the anisotropy [10].

The magnetoelastic energy corresponds to the mechanical energy that had to be supplied to the material to modify the pooling of electrons [10].

1.4 1.4. Magnetostatic energy

This energy corresponds to the action on each atom of the fields magnetic forces created by all neighboring atoms. The natural minimization of the sum of these different energies inside matter results in the appearance of elementary magnetic domains called “Weiss domains”. Pierre Weiss (1907), showed that a magnetized body is divided into domains within which the magnetic moments are ordered . Within these domains, the magnetization is oriented along directions imposed by the minimization of the different energies. They will mostly be close to the directions of easy magnetization. In the absence of an applied field and any other constraint, for a previously demagnetized material, there is equipartition of the volume of the domains between the various directions of easy magnetization and the resulting macroscopic magnetization is then zero [11].

1.4.2 Bloch walls

1.4.2.1 Origin of domains

The separation of the different elementary magnetic domains"Weiss domains" previously studied is materialized by what are called Bloch walls. These walls correspond to a magnetic zone where the magnetization passes from one direction to another. The distribution of the domains corresponds to an energy state minimal [12].

1.4.2.2 Types of walls

- ✓ The 180° walls separate two Weiss domains whose angle of the magnetization direction is 180° [12].
- ✓ The 90° walls separate two Weiss domains whose angle of the magnetization direction is 90° [12].

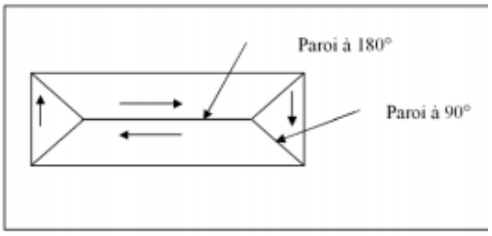

Figure I.8: Presentation of wall types [12]

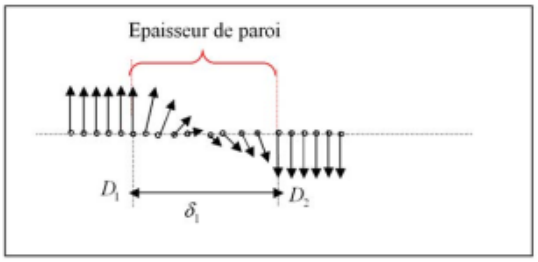

Figure I.9: Presentation of a 180° Bloch wall [12]

1.4.2.3 Wall characteristics

If **a** is the interatomic distance, and **n** the number of magnetic moments in the wall of thickness **δ** [13].

- ✓ Energy of the wall :

$$W_{ech} = \frac{1}{2} E \cdot m_i^2 \frac{\pi^2}{n} \qquad (I.14)$$

- ✓ Wall thickness:

$$\delta = \text{na} \qquad (I.15)$$

n: The number of magnetic moments.

a: The interatomic distance.

1.5 Ferromagnetism at different scales

As shown in (figure 1.5), ferromagnetism can be characterized at four different scales [14].

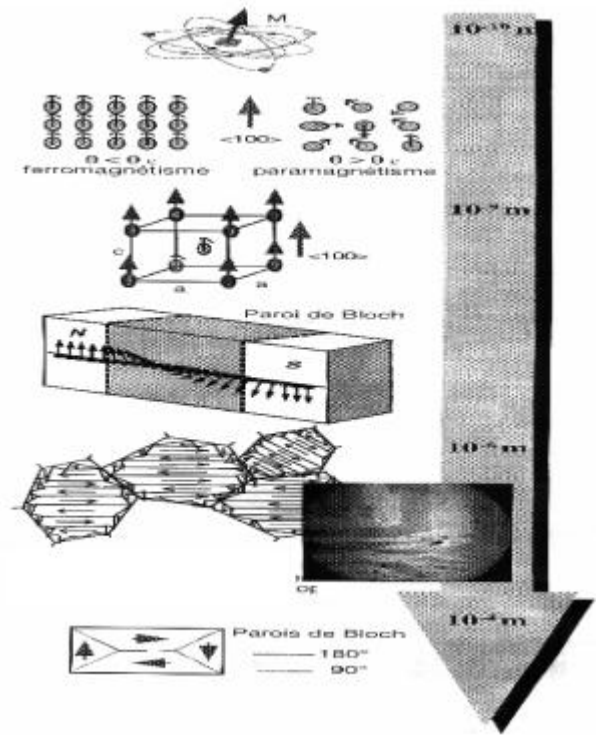

Figure I.9: Ferromagnetism at different scales [14].

1.5.1 At the atomic scale

A ferromagnetic material is distinguished by the existence of a strong permanent atomic magnetic moment [14].

1.5.2 At the crystalline scale

The energy responsible for the orientation of the magnetization along certain crystallographic directions is called "magnetocrystalline anisotropy energy" it is minimum in the direction of easy magnetization (axes which consume minimum anisotropy energy) in the case of a cubic symmetry, the axes of easy magnetization are the edges, i.e. the directions [001], [100], [010], while the diagonal [111] is of difficult magnetization [14].

I.6 Hysteresis

I.6.1.Definition

It is the response curve of the materials which represents the delay of the variation of the magnetic magnetization compared to the applied field [15].

I.6.2 Origin

It is a direct consequence of the existence of elementary domains and processes of magnetization by displacement and deformation of the Bloch walls in an anisotropic material [15].

Under the action of the magnetic field the volume of the oriented domains will increase in the direction of the field. This phenomenon occurs through a process of moving walls that requires little energy. During its displacement, a wall always remains parallel to an axis of easy magnetization, which means that when it disappears, the magnetization inside a grain is uniform. If the excitation field is increased, the magnetization of each grain rotates towards the direction of the excitation field until saturation [15].

I.6.3 Characterization

A material can be characterized by different plots and parameters. We distinguish: the anhysteretic curve, the first magnetization curve, the coercive field, the remanent induction and the saturation induction. As illustrated in the following figure (I-10) [15]:

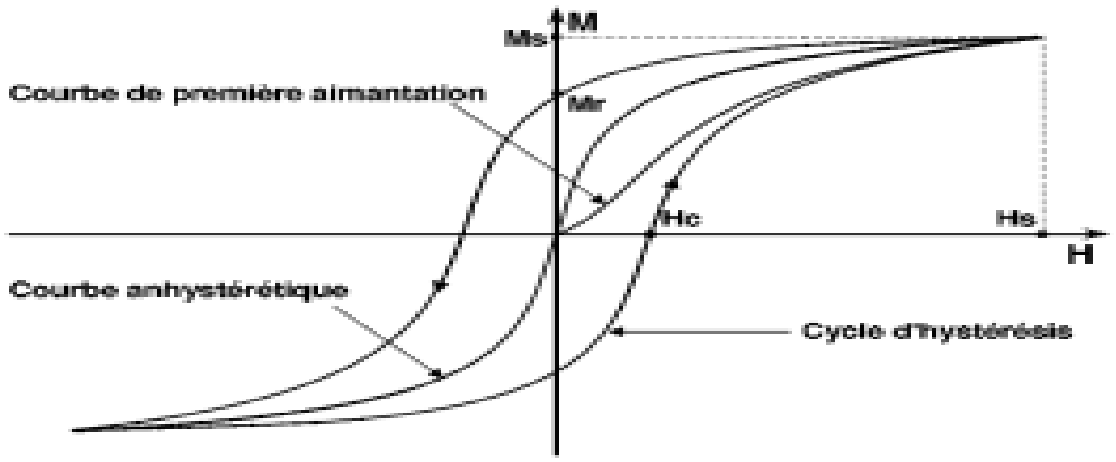

Figure I.10: hysteresis cycle and first magnetization curve
and anhysteretic curve [15].

II.6.3.1 Anhysteretic curve

The anhysteretic curve is the curve representing the induction as a function of the field as it would be if the transformations in the material were reversible, for which the walls occupy the position which corresponds to their minimum energy in the direction of the applied $\overrightarrow{H_0}$ field [15].

I.6.3.2. Curve of first magnetization

Called the first magnetization curve, it describes the evolution of the magnetization as a function of the field applied from the demagnetized state [15].

I.6.3.3. The coercive field

This quantity is the value of the external field capable of canceling the remanent magnetization [15].

I.5.3.4.Remanent induction

It is the value of the induction which remains even after the cancellation of the applied external $\vec{H}$ field [15].

I.6.3.5. Saturation induction

This is the maximum value that the induction can reach even if the external field applied is increased [15].

I.6.4.A hysteretic law

The resolution of the equations of the electromagnetic field is subordinated to the knowledge of a law linking the induction and the magnetic field, studies are carried out to achieve this. It is then necessary to go through the study of the mechanisms of hysteresis [16].

II.6.4.1. Hysteresis mechanism

For a material in the demagnetized state, each Weiss domain has a randomly oriented spontaneous magnetization with respect to its neighbors, which leads to zero macroscopic magnetization [16].

If a field is applied to a material, the distribution of the domains is modified by displacement of the walls and this results in a variation of the magnetization. If the field is weak enough, these wall displacements are reversible and therefore the variations in magnetization are reversible. If the applied field $\vec{\boldsymbol{H}}$ exceeds a certain critical value H_c, the displacements of the walls are then brutal and irreversible. If the applied field $\vec{\boldsymbol{H}}$ is sufficiently high, the magnetization increases by rotation of the Bloch domains and tends to reach a

maximum magnetization which is the saturation magnetization M_s, all the spins are parallel [16].

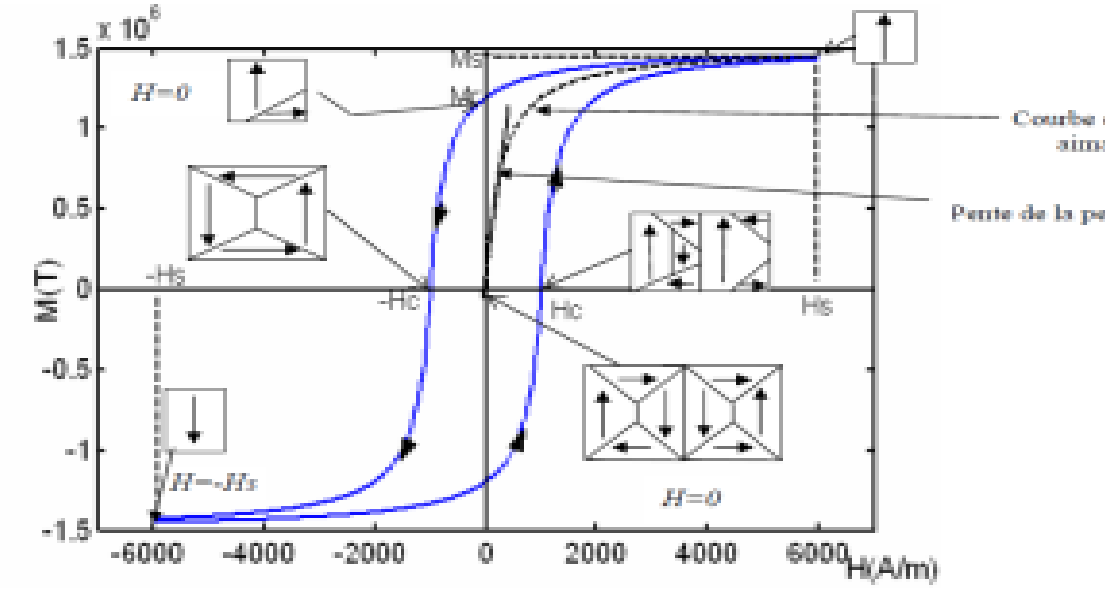

Figure I.11: diagram explaining the mechanism [16].

I.6.5.Cycle types

I.6.5.1.Cycle majeur

the CDEFGHC cycle which is the normal hysteresis cycle [16].

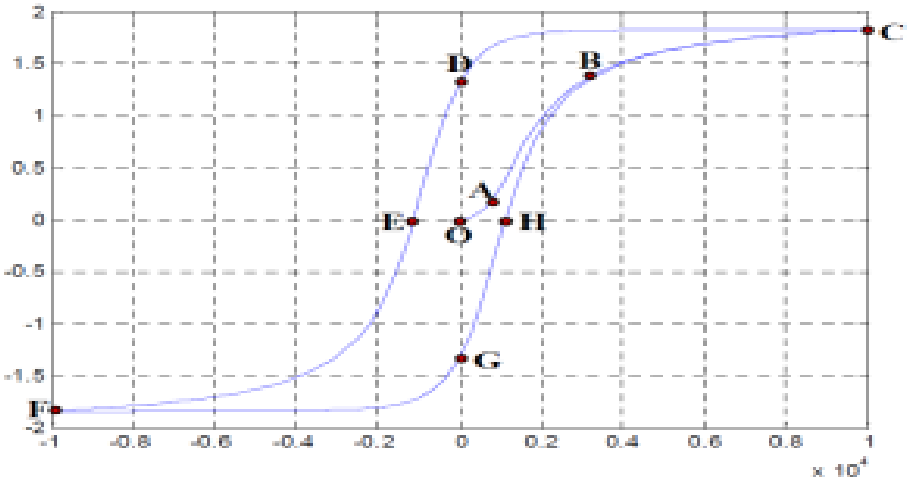

Figure I.12: hysteresis cycle [16]

II.6.5.2.Centered and non-centered minor cycle

This is the hysteresis cycle obtained during field decrease without reaching saturation. The non-centered hysteresis cycle is obtained by inverting the field between two values lower than that of the maximum field in modulus, it is therefore not centered around the origin [16].

I.6.6. Bruit BARKHAUSEN

I.6.6.1 BARKHAUSEN experiment

A magnet rotates slowly, inducing in a ferromagnetic bar a reversal of Polarization according to a periodic movement, the period is approximately 1s, a winding picks up the variations of magnetic flux in the bar, which are transmitted after amplification to a loudspeaker [17].

Normally no audible sound should be emitted, but each time the polarization is reversed, a noise reminiscent of the flow of small grains in a container is heard, this problem demonstrates that under the effect of a sufficiently large external field [18].

The polarization is not done continuously, but by small successive jumps [18]:

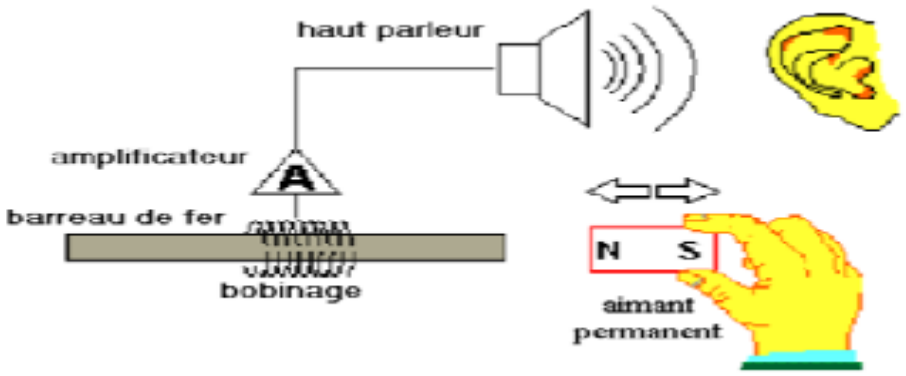

Figure I.13: BARKHAUSEN experiment [19]

In order to explain this character, it is necessary to imagine the interaction of crystalline and magnetic microstructures. The crystal can contain a large number of imperfections, precipitates, vacancies, dislocations and grain boundaries, to generalize all that can alter the perfection of the crystal lattice [19].

Arriving on a defect, the wall will block and remain anchored, if the applied field increases, the wall will suddenly detach to reach a new defect [19].

The ability of defects to block a wall depends on their nature and the interaction energy that exists between them and the wall [19].

I.6.6.2 Discontinuity of the magnetization process

As described previously, the domain structure is established spontaneously to reduce the total energy of the system. The application of an external field causes a modification of

organization essentially due to the displacements of the walls limiting the domains, so that well oriented, they increase in volume to the detriment of those badly oriented. Indeed, the walls do not move freely, they are slowed down by the impurities present in the material. This corresponds to a phenomenon of anchoring of the walls, the displacement of the latter being discontinuous, it is then done by jumping. The walls are torn from the anchors to be blocked on new obstacles and so on [19].

I.6.6.3 BARKHAUZEN Noise Measurement

Each jump of a Bloch wall induces an electromagnetic disturbance, a coil (probe) judiciously placed and oriented on the material makes it possible to transform the flux variations induced by the disturbance into voltage pulses, each BARKHAUZEN event in the material induced a voltage pulse across the receiving coil and the sum of all these events form what is called "BARKHAUZEN noise" whose intensity depends on the applied field and the capacitance of the faults [19].

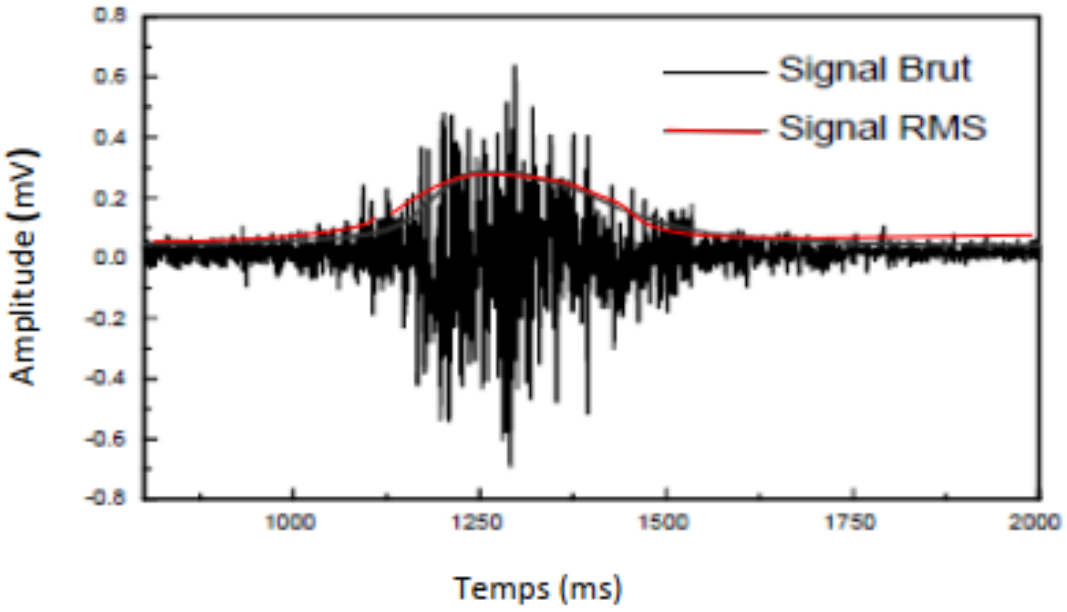

Figure I.14. Example of Raw BARKKAUSEN Noise and RMS [19].

I.6.6.4. Applications of the BARKHAUSEN effect to the monitoring of microstructural evolutions

The equilibrium state of a ferromagnetic material corresponds to the minimization of all energies (exchange energy, magnetocrystalline anisotropy energy, etc.). The sensitivity of the

magnetic behavior to external parameters is always explained by a modification of this balance [20].

- **a. Influence of microstructure**

The effects of the microstructure on the BARKHAUSEN signal are illustrated in Figure 13 which represents the responses corresponding to three classic constituents of steels such as ferrite (steel at 0.1% carbon, annealed state), pearlite (steel at 0.8% carbon, annealed condition), martensite (0.55% carbon steel, tempered condition after austenitization at 875 C° [20].

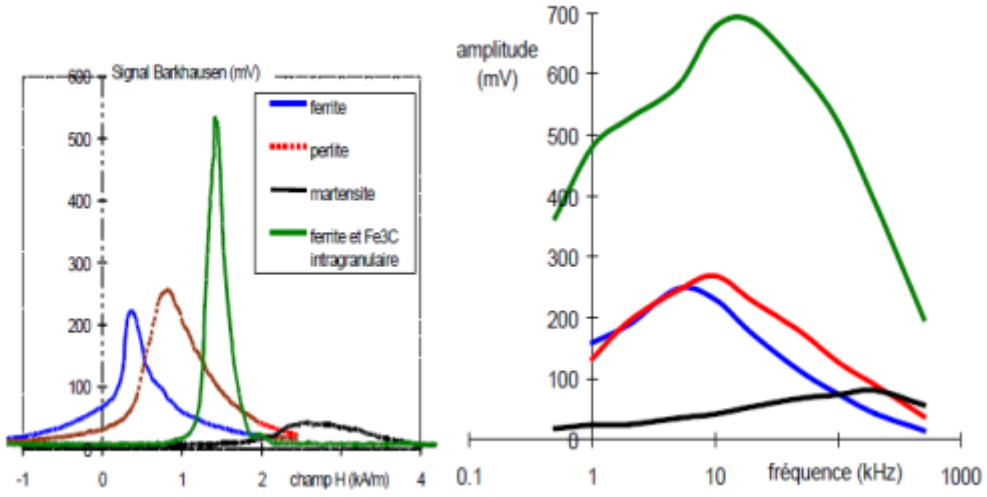

Figure I.15 : BARKHAUSEN signals and frequency analysis for different metallurgical states [20]

We observe for each sample very different responses in terms of position and amplitude of the peak [20].

- ✓ For ferrite the maximum response appears for a weak magnetic field.
- ✓ Perlite has a similar shape but centered around a more intense field, this difference is explained by the more numerous obstacles which slow down the movements of the walls in the case of perlite.
- ✓ The martensitic peak is not very intense and is located towards high fields [20].

- **b. Influence of grain size**

Most of the research teams that have studied the BARKHAUSEN noise report that the RMS amplitude of the BARKHAUSEN signal decreases when the grain size increases, and that the amplitude of these signals

increases for large grain sizes, these results indicate that during magnetization, wall displacements would be longer but less numerous, which would justify the reduction in the amplitude of the RMS signal [20].

- **c . Influence of precipitation**

Precipitation will also influence BARKHAUSEN noise measurements, the effect of precipitation varies according to the size of the precipitates. When the size of the precipitates is of the order of magnitude of the thickness of the walls about 0.03µm, the influence on the BARKHAUZEN noise is maximum. And if the precipitates are larger in size, the precipitates will only play the role of nucleation site for closure domains [21].

- **d. Stress state influences**

BARKHAUSEN noise is also very sensitive to applied or residual stresses. the plastic deformation introduced into the material crystalline defects that will modify the magnetic structure but also play the role of obstacles to the walls of Bloch. Thus the presence of dislocation magnetically hardens the material. On the other hand, the elastic deformation of the network changes the magnetostriction energy and thus the magnetic microstructure. The BARKHAUSEN noise measurements carried out on various steels show that ,for a measurement of the BARKHAUSEN signal with a magnetisation in the direction of the stress [19]:

- ✓ In tension, the amplitude of the BARKHAUSEN peak increases.
- ✓ In compression, not only does the amplitude of the peak decrease, but we also observe the appearance of shoulders on either side of the BARKHAUSEN peak, attributed to the movement of the walls at 90° [19].

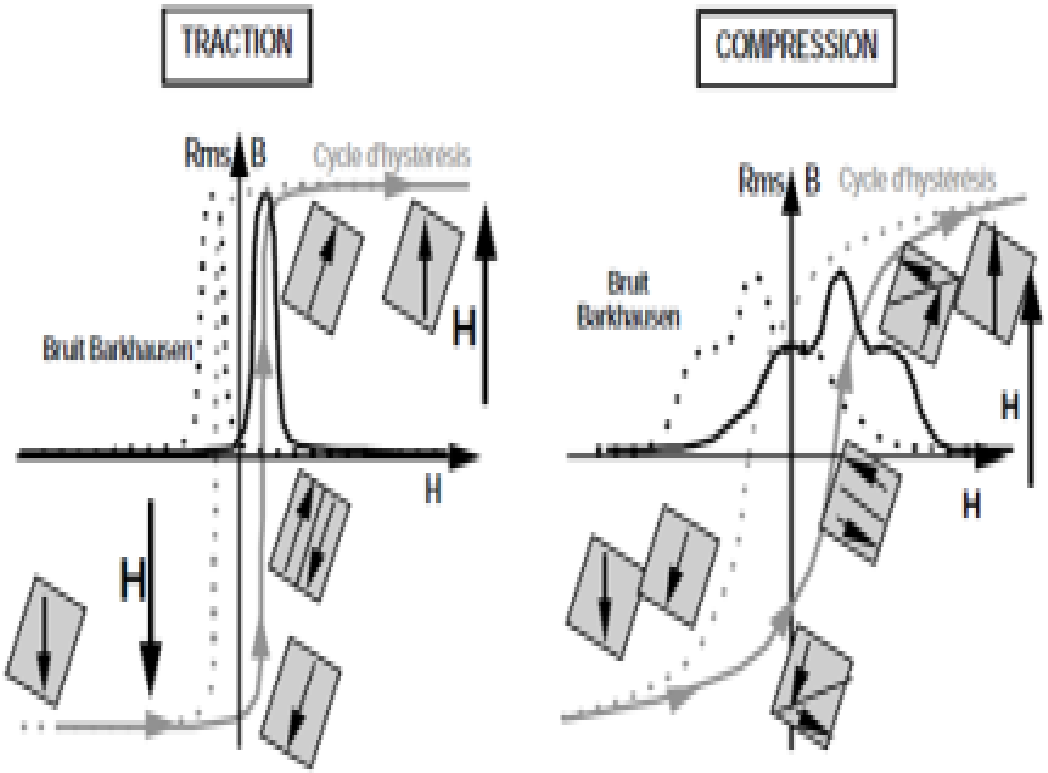

Figure I.16 : Qualitative explanation of stress sensitivity [20].

I.6.7 Different devices used in the BARKHAUSEN noise technique

I.6.7.1. 3MA: « Micromagnetic Multiparameter Microstructure and Stress Analysis »

The first generation of 3MA equipment relied solely on BARKHAUSEN magnetic noise and tangential magnetic field analysis. In 2007, there were more than 100 facilities used in different industrial areas, it mainly covers steel building and machinery industries. Today, 3MA equipment is in its fourth generation. Compared with BARKHAUSEN magnetic noise (MBN) based micromagnetic testers, only 3MA uses three other micromagnetic and electromagnetic methods in addition to MBN analysis in order to obtain more material information [22].

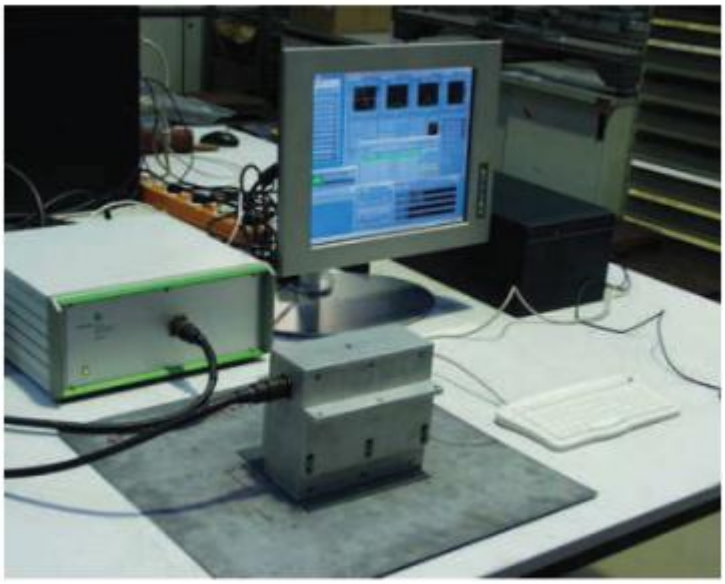

Figure I.17: 3MA hardware and software based on TCP-IP controlled by a PC [22]

I.6.7.2 MikroMach: «Mobil Micro Magnetic Analysis and Characterization »

The MikroMach Device is a handheld device, which consists of a "Yoke", a "Solenoid" excitation coil, a "Sensor" Hall effect sensor, an energy generator and of the corresponding electronics and is connected to a portable computer from which the device is controlled and the data is processed and visualized [23].

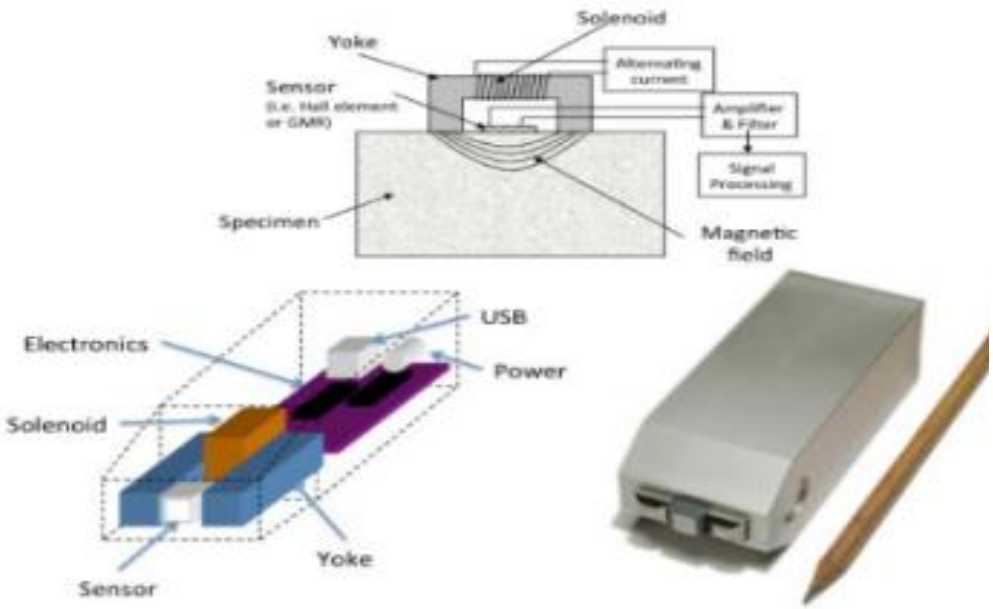

Figure I.18: MikroMach system for electromagnetic characterization [23]

I.7 Conclusion

The magnetism of the material is the consequence of the movements of the electrons gravitating around the nucleus of the atoms of this material, in the absence of the exciting magnetic field, the atomic magnetic moments are locally oriented in the same direction, each region where the moments have the same orientation is a magnetic domain (Weiss domain), the area of transition between two domains is a Bloch wall. In the absence of an exciting magnetic field, the vector sum of the magnetic moments is zero.

But in the presence of an exciting field there is displacement of the Bloch walls and crossing of the best oriented domains to the detriment of the others. Saturation is reached when the single crystal (or grain) consists of a single domain oriented in the direction of the exciting field.

The magnetization of a ferromagnetic material from saturation to saturation as we have described it is done by modification of the magnetic microstructure. The phenomenon of magnetostriction intervenes in this process.

We notice a very high sensitivity of the BARKHAUSEN noise to the different parameters of the crystalline microstructure of the steels. Moreover, this technique seems to be able to provide separate information between the different elements (precipitates, grain boundary) or the different constituents.

References

[1] Pierre HOUSSIN, Georges WESSELS, Des matériaux (Jean-Paul Bailon).

[2] laboratoire mécanique Alfa pipe Ghardaïa.

[3] H.Bouhafs, "Contribution à l'étude des causes de dégradation des conduites du transport d'eau industrielle", Mémoire de Master, université Badji Mokhtar, Annaba, 2016.

[4] Y.Barkat, "Étude comparative entre deux procédés de soudage des pipelines**"**, Mémoire de Master, Université de Biskra, 2016.

[5] A.Debabi, "Etude des caractéristiques mécaniques d'un joint de soudure après application d'un traitement thermique", Mémoire de Master, Université Mohamed Boudiaf**,** M'SILA, 2018.

[6] K.Hulka,"HSLA large diameter pipe plate from standard production to X80/X100", Niobium Information 13/39, 1997.

[7] "High strength structural and high-strength lowalloy steels", Metals Handbook**,** Tenth edition, 1990.

[8] Y.Bouguerra et S.Bourahla, "Analyse structurale de l'acier XC42 du point de vue fissuration à froid en soudage", Mémoire de Master, Université Mouloud Mammeri, Tizi Ouzou, 2017.

[9] A.Pineau, "Intégrité mécanique des pipelines et gazoducs: enjeux scientifiques et techniques". Séminaire International sur les Technologies Mécaniques : SITEM 09, Tlemcen, 05 et 06 Décembre 2009.

[10] F.Khamouli, " Influence du flux de soudage sur la qualité de la soudure des Pipelines", Thèse de Doctorat, Université Badji Mokhtar, Annaba, 2018.

[11] V.Smanio-Renaud, "Etude des mécanismes de Fragilisation Par l'Hydrogène des aciers non alliés en milieu H2S humide: contribution de l'émission acoustique", Thèse de Doctorat, l'Institut National des Sciences Appliquées, Lyon, 2008.

[12] Mechanical Metallurgy, G.E.Dieter, chap.9, The Tension Teste, p.329-377, Internatl, Student Edition McGraw-Hill, 1976.

[13] American Petroleum Institute, (2004), "API Specification 5L", 42nd ed, Washington, D.C, 2004.

Chapter II Steels

II.1. Introduction

Due to its physical, chemical and mechanical properties, steel occupies an important place in the ferrous metals industry, hence its use in various fields such as in the pipeline transport of hydrocarbons (oil and natural gas). It is used for the manufacture of pipelines (gas pipelines and oil pipelines) to transport large quantities of hydrocarbons over long distances from their deposits to consumption and processing areas. Today there are more than one million km of pipeline network in operation in the world. The network in Algeria is estimated at more than 16,000 km for diameters ranging from 8 to 48 inches. For their efficiency, these pipes must meet profitability and safety requirements. More than 95% of the steels used for gas pipelines are high-strength micro-alloy steels. They are obtained by increasingly efficient metallurgical schemes by increasing the cooling rate after controlled rolling, such as TMCP (Thermo Mechanical Controlled Process) sheets obtained by rolling at a controlled temperature followed by accelerated cooling [1].

Pipes buried in the ground are subject to significant stresses and a corrosive environment. For this, the development of new HSLA steels (HLE) has been oriented towards a modification of the mechanical properties in order to avoid an excessive increase in the thickness of the tubes. We managed to obtain a compromise between a high elastic limit to withstand high pressures and good toughness to resist the propagation of cracks thanks to the development of TMCP sheets. Steels have gone from grade X52 to grade X70 used today with ferritobainitic microstructures. The transition to higher grades X80, X100 requires the development of steels with ferritobainitic structures [1].

We will present in this second chapter, the material of study, the chemical compositions, the structures and the mechanical properties [1].

Figure II.1: Pipeline in the environment [2]

II.2. The Steels

II.2.1. Definition

Steel is an iron alloy containing less than 2% carbon. It can be listed according to this carbon content which fixes its level of maximum hardness in the quenched state. A high carbon content steel will be used for its high hardness while a lower content steel is less hard and more malleable. It generally contains small quantities of other elements in addition to iron and carbon, incorporated, voluntarily or not, during its elaboration. One can also add larger quantities of alloying elements , figure II.2 presents the unit cells of the crystalline structures (C.C and C.F.C) [3].

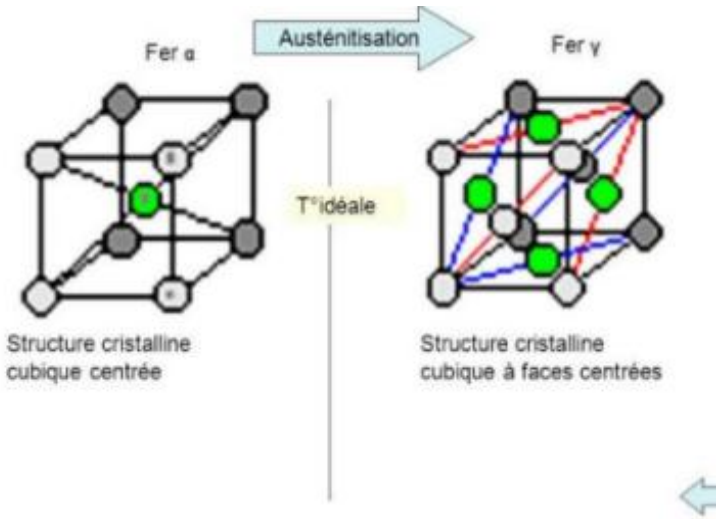

Figure II.2: Unit cells of crystal structures (C.C and C.F.C) [4]

I.2.2. Types of steels

The steels were classified according to two criteria, the composition and the level of quality. Thus, a distinction is made between non-alloy (<1% alloy), low-alloy (content of each alloy element <5%) or high-alloy ≥5% steels. Depending on the guarantee given to the properties of use, basic steels, quality or special steels. The latter are placed in three families : [5]

- ✓ engineering steels (low or unalloyed).
- ✓ tool steels (low or high alloy).
- ✓ stainless steels.

The oil and gas industry, which is the driving force of the world economy, requires metallurgists to provide steels with a good combination of strength, toughness and weldability for the transportation needs of their products [5].

These criteria have led to the development of low carbon steels called HSLA (high tensile steel) [5].

High strength low alloy (HSLA) steels are a group of low carbon steels that use few alloying elements to achieve yield strengths higher than 275 MPa in the rolled or normalized condition [5].

These steels have better mechanical properties and sometimes improve corrosion resistance than rolled carbon steels. Moreover, because the high yield strength of HSLA steels can be obtained at low carbon content, the weldability of HSLA steels is comparable or better than that of mild steels [6].

II.2.3 HSLA steels (High-strength low-alloy)

HSLA steels have been developed in a wide range of yield strength, from 315 to 700 MPa level in hot rolling and from 240 to 355 MPa level in cold rolling [7].

These are mild and extra mild steels to which small quantities of elements are added, in particular (Nb, Ti, V, Al) in order to trap Carbon and Nitrogen in the form of carbides and nitrides, and for this are called micro-ally steels [7].

H.S.L.A steels can be divided into six categories [5]:

- ✓ Corrosion resistant steels.
- ✓ Ferrito-pearlitic steels.
- ✓ Laminated steels with a pearlitic structure.
- ✓ Acicular ferrite steels.
- ✓ Dual-phase steels.
- ✓ Control inclusion form steels.

I1.2.3.1 Corrosion resistant steels

The first HSLA steels developed were the corrosion resistant steels. These steels contain copper and other elements which increase corrosion resistance, solution-solid hardening and some grain refinement of the ferrite microstructure. The hardening effect of several alloying elements is shown in Figure II.3 [5].

Vanadium and/or niobium can improve the yield strength of these steels; addition of niobium also improves hardness. Normalizing or controlled rolling and cooling can also refine grain size (and thus improve hardness and yield strength). However, if normalization or accelerated cooling are employed to refine grain size, the effect of carbon and contained microalloying elements on hardenability and the potential for undesirable transformations to higher bainite and Widmanstätten ferrite should be considered [5].

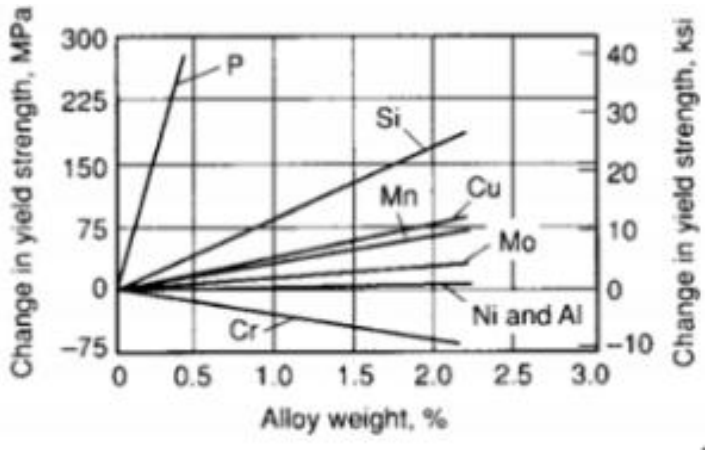

Figure II.3. Solution-solid hardening of ferrite [5].

I1.2.3.2 Ferrito-pearlitic steels.

These steels employ additions of micro alloying elements such as niobium and vanadium to increase the yield strength of hot rolled steel without high carbon and/or manganese content. Structural material properties resulted from the discovery that a very small amount of niobium and vanadium (< 0.10%) strengthens carbon-manganese steels without interfering with subsequent processing. The carbon content could be reduced in this way to improve weldability and hardness because the hardening effects of niobium and vanadium compensated for the reduction in hardness due to the reduction in carbon content [5].

The development of rolling processes coupled with chemical composition has produced high yield strength accompanied by a gradual lowering of the carbon content. Many of the HSLA class of microalloyed steels have carbon content as low as 0.06% or even lower, yet they can still develop yield strengths of 485 MPa. The high yield strength is achieved by the combined effects of fine grain size developed during hot rolling and precipitation hardening that is due to the presence of vanadium, niobium, and titanium [5].

Les divers types des aciers micro alliés ferrito-perlitique incluent [5]:

- ✓ Steels micro alloyed with vanadium

- ✓ Micro niobium alloy steels
- ✓ Steels micro alloyed with niobium-molybdenum
- ✓ Steels micro alloyed with niobium-vanadium
- ✓ Steels micro alloyed with vanadium-nitrogen
- ✓ Titanium micro alloy steels
- ✓ Micro-alloy niobium-titanium steels
- ✓ Steels micro alloyed with vanadium-titanium

These steels may also include other elements for corrosion resistance and solid solution hardening, or to increase hardenability (if transformation products other than ferrite-pearlite are desired) [5].

I1.2.3.3 Laminated steels with a pearlitic structure

Pearlitic rolled structural steels are a specific group of HSLA steels having increased mechanical properties (and, in some cases, atmospheric corrosion resistance) obtained by the addition of moderate amounts of one or more microalloying elements. other than carbon. Some of these steels are manganese carbon steels and differ from ordinary carbon steels only by having a higher manganese content. Other pearlitic structural steels contain small amounts of alloying elements, which are added to increase weldability, formability, hardness, and toughness [5].

Pearlitic rolled structural steels are characterized by yield strengths in the range of 290 to 345 MPa. They are not intended for hardening and should not be subjected to such treatment. For some applications, they may be annealed, normalized, or stress relieved, processes which may change mechanical properties [5].

When these steels are used in welded structures, care must be taken in the selection of grade and in the specification of welding procedure details. Some categories can be welded without preheating or postheating. The basic disadvantages of these steels is that the pearlitic microstructure increases the transition temperature but does not improve the yield strength. [5]

I1.2.3.4 Acicular ferrite steels

Another approach to the development of HSLA steels is to achieve a very fine, high strength needle-like ferrite microstructure, instead of the usual polygonal ferrite microstructure, during the cooling transformation of ultra low carbon steels (< 0.08% C) with sufficient hardenability (by additions of manganese, molybdenum, and/or boron). Niobium can also be used for precipitation hardening and grain refining. The main difference between

the structure of acicular ferrite (also referred to as low carbon bainite) and that of polygonal ferrite is that the former is characterized by a high dislocation density, and the fine grains strongly ovals that are not exhibited in polygonal ferrite [5].

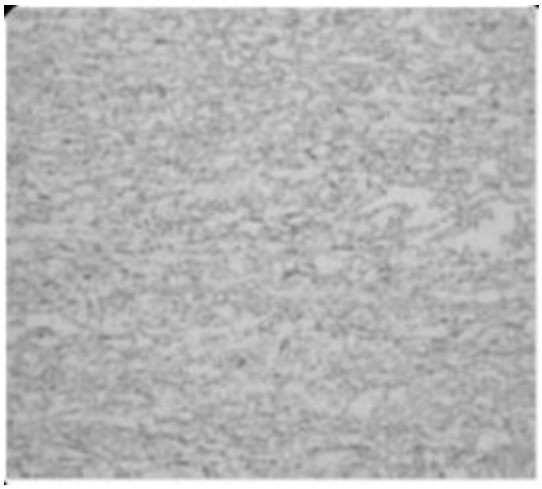

Figure II.4. Microstructure of acicular ferrite HSLA steel [5].

Acicular ferrite steels can be obtained by quenching or, preferably, by air cooling with the appropriate alloys for hardenability. The main advantage of this type of HSLA steel is the unusual combination of high yield strength (415 to 690 MPa), high toughness figure (II.5.), and good weldability. An important application of these steels is pipelines. The properties of a rolled needle ferrite steel are summarized in figure (II.5.), The main application of needle ferrite steel involves hydrocarbon pipelines in arctic conditions. This application requires a combination of superior hardness, high strength, excellent resistance to hydrogen induced cracking and class leading field weldability [5].

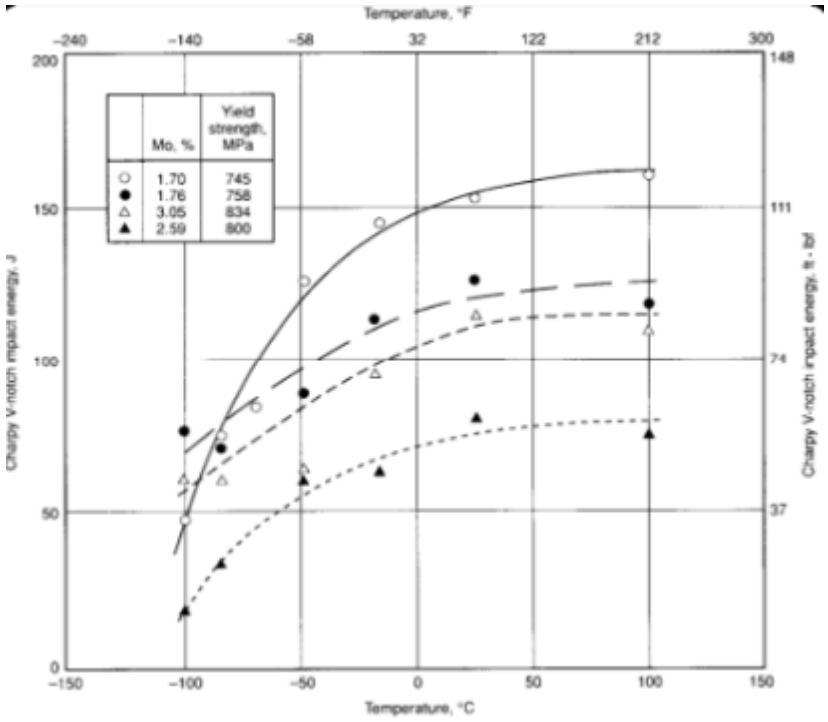

Figure II.5. The impact strength and yield strength of a 25 mm rolled steel at an ultra low carbon bainitic structure. Nominal grades of alloying elements included 0.024 to 0.027% C, 0.92 to 1.00% Mn, 3.54 to 3.63% Ni, and 0.050 to 0.055% Nb [5].

In response to these needs, researchers have developed a steel of hard needle-like ferrite for pipeline by optimization of carbon and niobium content, addition of boron, and/or application of accelerated in-line cooling [5].

In this pipeline, the optimum carbon content ranges from 0.01 to 0.05%. Below 0.01% carbon, the grains of the heat affected zone (HAZ) close to the molten zone are embrittled, because of the intergranular cracking induced by hydrogen and the loss of hardness in the HAZ. The addition of boron and/or the application of accelerated in-line cooling provides superior hardness and high strength, with desirable weld characteristics. Three categories for Arctic service are available: X-65, X-70, and X-80. An X-70 composition includes 0.03% C, 0.25% silicon, 1.91% manganese, 0.008% P, 0.001% S, 0.048% N, plus titanium, boron, and calcium [5].

I1.2.3.5 Dual-phase steels

These steels have a polygonal (80-90%) ferrite microstructure and 10-20% martensite islands scattered throughout the ferrite matrix. the term dual phase refers to the predominance in the microstructure of two phases, ferrite and martensite. These steels have a low yield strength and a tensile strength of approximately 550 MPa [5].

Dual-phase steels can be produced from low carbon steels in three ways [5]:

- ✓ Intercritical austenitization of carbon-manganese steels followed by rapid cooling.
- ✓ hot rolling with elements favoring the formation of ferrite such as silicon and elements which delay the transformation such as chromium, manganese, and/or molybdenum.
- ✓ Continuous annealing of cold rolled carbon-manganese steel followed by quenching and softening.

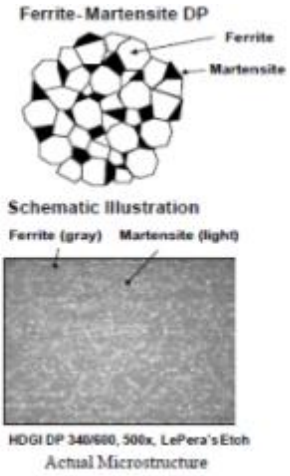

Figure II.6. Microstructure of a dual phase steel [5]

I1.2.3.5 Control inclusion form steels.

An important development in microalloyed HSLA steels is the use of inclusion shape control. Sulphide inclusions, which are plastic at rolling temperatures and so elongate and flatten during rolling, adversely affecting ductility in the short transverse direction (through thickness). The main objective of inclusion shape control is to produce sulfide inclusions with negligible plasticity even at the highest rolling temperatures [5].

I.2.4 Pipeline steel tubes :

A pipeline (originally from English) is a pipe formed by a set of butt-welded steel tubes, intended for the transport from one place to another of gaseous or liquid materials. These tubes are often coated externally and even internally and almost always buried except in certain regions [8].

A pipeline allows the exchange of products between refineries, oil depots and port facilities. Its length can vary from a few kilometers to hundreds of kilometers, even thousands of kilometers [8].

Depending on the product being transported, the pipelines are named differently. Their construction and operating techniques differ according to certain regulations [8].

The main pipeline transport systems relate to [8]:

- ✓ Gas pipelines for transporting natural gas.
- ✓ Pipelines for transporting petroleum and liquid hydrocarbons.
- ✓ Aqueducts (canals) pipes or outfalls used for fresh water and irrigation.

Figure II.3 : Pipelines [9].

I.2.5. Steels used to manufacture pipelines:

The long-distance transport of large quantities of hydrocarbons required the use of high-strength tubes capable of withstanding very high pressures [10].

New grades with improved mechanical properties have been used. This is how we saw the appearance of the X60, X65, X70, X80 and even X100 shades [10].

The types of steels used for tubes can be divided into two groups [10]:

- ✓ low alloy carbon steels.
- ✓ low carbon steels.

In the first group, we find the so-called ferritic-pearlitic steels such as X42 to X52 according to API standards, containing up to 0.3% C, 1.6 % Mn, 0.7 % Si b [10] .

In the second group we find ferritic-pearlitic steels weakly microalloyed with lower carbon content such as: X56, X50, X65, X70 and X80 containing 0.12%C, 0.45%Si, 0.25%S , 1.9%Mn, 0.1%V, 0.1%Nb, 0.015%Al [10].

For pipes with a diameter greater than 1020 mm, intended to operate under high pressures, steel tubes obtained by controlled rolling are generally used [10].

The mechanical properties can be modified by adjusting the structure by refining, among other things, the structure of the rolled sheets (refining of the grains). This method is recognized as making it possible to improve both the tensile characteristics Re and/or R, as well as the transition temperature. In recent years, the controlled rolling process has been supplemented by accelerated cooling, spraying with water at sufficiently high cooling rates [Bou07], in order to improve the mechanical characteristics of the sheets, thus making it possible to increase the resistance. steel up to 700 MPa [10].

II.3. API 5L X70 Steel :

II.3.1. Definition:

The steel studied is taken from an API 5L X70 PSL2 SAWH type steel tube intended for the pipeline of natural gas for the GR7 project [11].

The meanings of these latter designations are as follows [11]:

- ✓ API: American Petrolium Institute
- ✓ 5L: Specification for the pipeline
- ✓ X: Grade designation for high strength pipeline
- ✓ PSL2: the specifications are in the form of intervals
- ✓ SAWH: Submerged Arc Wilding Helical

The number after the "X" corresponds to the value of the minimum elastic limit. For example X70 has a minimum yield strength of 70 ksi (Min=485 Mpa) [11]

The nominal thickness of the studied tube is 12.95 mm and has a diameter of 48" (1219.2mm) with a variable length [26].

II.3.2. Microstructure of API5L X70 steel:

The X60, X65, X70 type steels present a microstructure of the ferrito-pearlitic type, the pearlite bands marked in the X60, X65, X70 type steels explain the sensitivity of these steels to cracking. This banded microstructure promotes crack propagation [12].

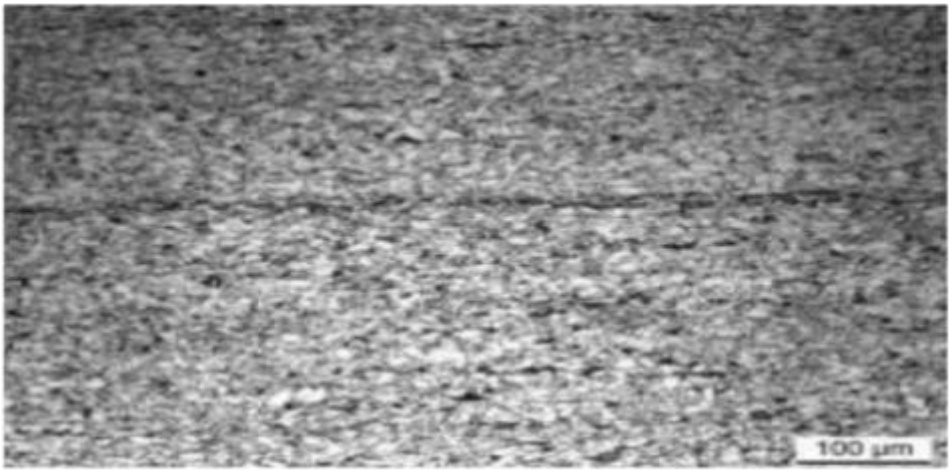

Figure II.2: Ferrito-pearlitic microstructure of API 5L X70 steel [11]

II.3.3 Microstructure of API5L X70 steel:

The grades of steel commonly used in the construction of pipelines are defined in two API [American petroleum Institute] specifications which have been adapted since 1922 by the American petroleum industry (Called 5L for normal grades) 5L , for grades high resistance. These specifications are in general use around the world. The most used grades of steel have the mechanical properties presented [13].

Table II.1 Propriétés mécaniques des aciers pour tubes selon la norme API [13]

SPECIFICATION API	GRADE	ELASTICITY LIMIT (kg/mm2)	RESISRANCEA LARUPTURE (kg/mm2)
5L	A	21	34
5L	B	25	42
5LX	X42	29	42
5LX	X46	32	45
5LX	X52	37	47
5LX	X56	39	52
5LX	X60	41	55
5LX	X65	46	56
5XL	X70	48	56

II.3.4 API-5L standard :

For more than 25 years, the metallurgy and steel industries have been developing new types of steels, called High Elastic Limit Steels (HLS steel), in order to reduce the cost price of pipelines. These metals, which have good mechanical properties, make it possible to reduce the thickness of the pipelines, thus minimizing the quantity of material necessary for their development. Since the manufacturing cost of a pipeline is essentially determined by this quantity, the use of HLE steels allows significant savings to be made [13].

The following four tables reflect the chemical composition of API 5L type steel, PSL1 and PSL2 line pipes [13]:

Table II.2 Chemical composition % (welded PSL1 line pipes) [13]

API 5L - PSL1	Carbone C (max)	Manganèse Mn (max)	Phosphore P (max)	Soufre S (max)	Titan Ti (max)
X42	0.26	1.30	0.030	0.030	0.04
X52	0.26	1.40	0.030	0.030	0.04
X60	0.26	1.40	0.030	0.030	0.04
X65	0.26	1.45	0.030	0.030	0.06
X70	0.26	1.65	0.030	0.030	0.06

Table II.2 Chemical composition % (welded PSL2 line pipes) [13]

API 5L - PSL2	Carbone C (max)	Manganèse Mn (max)	Phosphore P(max)	Soufre S (max)	Titan Ti (max)
X42	0.22	1.30	0.25	0.15	0.04
X52	0.22	1.40	0.25	0.15	0.04
X60	0.22	1.40	0.25	0.15	0.04
X65	0.22	1.45	0.25	0.15	0.06
X70	0.22	1.65	0.25	0.15	0.06
X80	0.22	1.85	0.25	0.15	0.06
X100	0.22	1.85	0.25	0.15	0.06

II.3.5 Phase diagram:

The equilibrium diagram is a graphical representation indicating the composition of the phases and the structure of the Fe-C alloy, produced under ordinary pressure assuming extremely low heating and cooling rates [14].

The solubility domains of carbon are denoted by γ and α respectively, the solubility being very low in the α state unlike the γ state which is larger, which explains the extent of the γ domain compared to the α domain which is extremely reduced [15].

Probably the most important of all the binary alloy systems is that of iron and carbon. Steels and cast irons, essential structural materials in any technologically advanced society, are essentially iron*carbon alloys. This section focuses on the study of the equilibrium diagram of this system and on the formation of several possible microstructures [16].

This diagram is very important for the operations of production, forming, welding, and heat treatment of steels and cast irons. Before using it, it is necessary to fully understand each region [17].

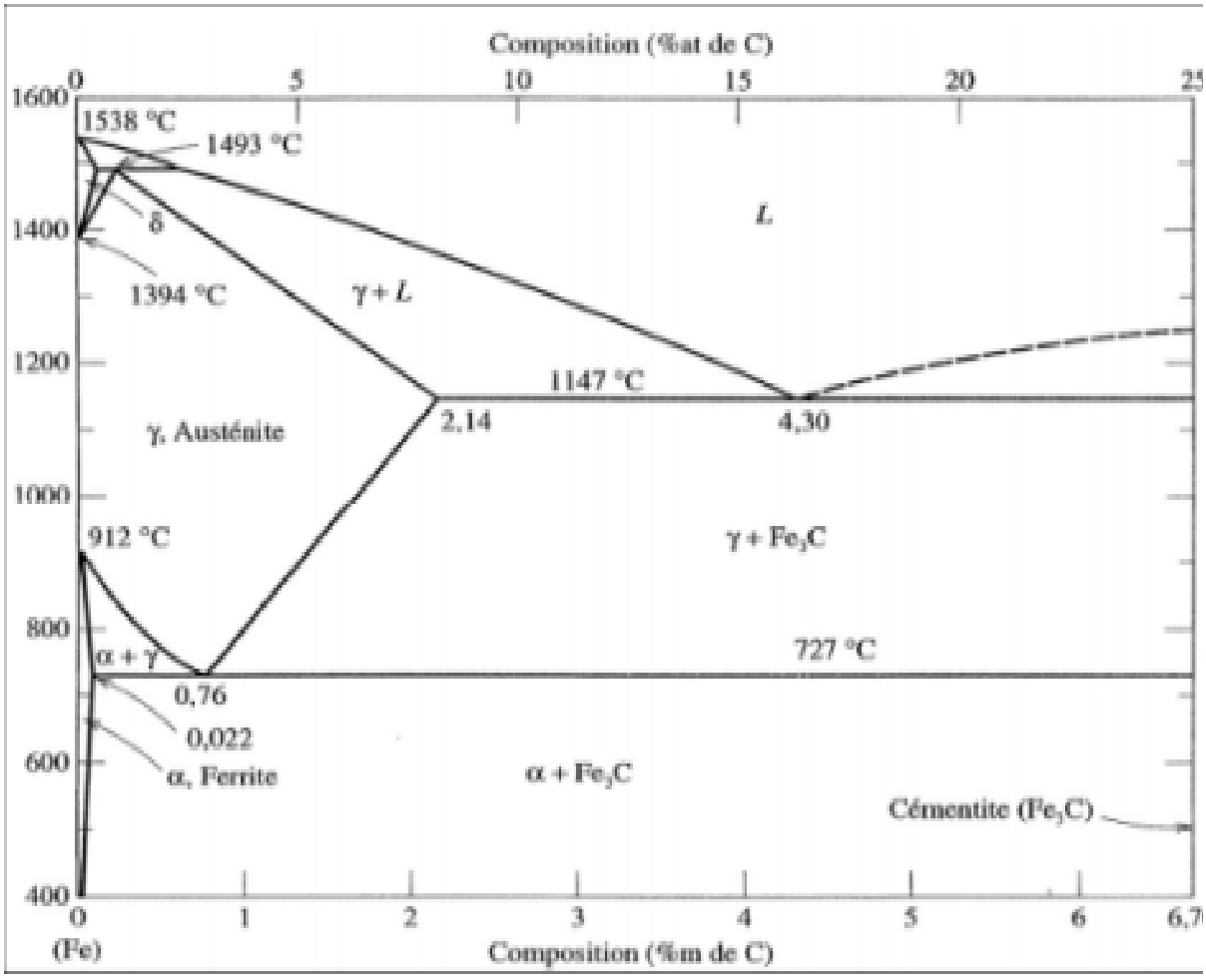

Figure II.3: Metastable or cementite Fe-C equilibrium diagram [18].

 Iron: %C < 0.008%, α phase [18].

 Steels: %C < 2.14%, α phase and Fe3C [18].

In practice : %C < 1%

- ✓ For a eutectoid steel (%C = 0.76), solid austenite γ is completely transformed into pearlite (α +Fe3C) [17].
- ✓ For a hypoeutectoid steel (%C < 0.76), solid γ austenite is transformed into α+ (α+Fe3C) [17].
- ✓ For a hypereutectoid steel (%C > 0.76), solid austenite γ is transformed into pearlite (α+Fe3C) + cementite (Fe3C) [17].

 Cast irons: 2.14% < %C < 6.70%, α phase and Fe3C [18].

In general: 2.14% < %C < 4.5%.

II.3.5.1 The main phases of phase diagram

- **Ferrite**

This phase contains a very small amount of carbon. Ferrite is also known as α ferrite or α iron. This phase contains a maximum of 0.02% carbon at 727°C (1341°F). As the temperature increases to 912°C (1674°F), the carbon content in the ferrite tends towards zero. Also, when the ferrite is cooled to room temperature, the amount of carbon decreases. The formation of ferrite begins as soon as a steel or cast iron is cooled below 727°C (1341°F). The ferritic structure is centered cubic and is both ductile and tough (figure II.4) [17].

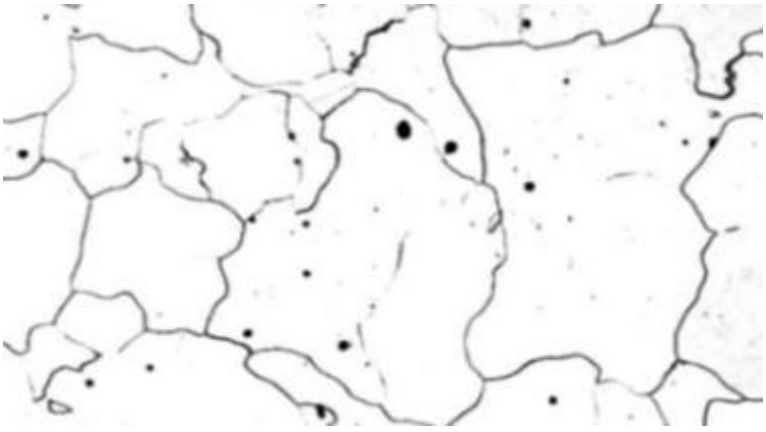

Figure II.4 : Structure ferritique [17].

- **Cementite**

Pure cementite has the molecular formula Fe3C. It contains 6.69% carbon, because of this high carbon content, pure cementite is not shown in Figure II.5. As mentioned before, a high carbon concentration is accompanied by an increase in hardness and brittleness. Cementite, with its high carbon content, is hard and brittle. This phase is also known as iron carbide [13].

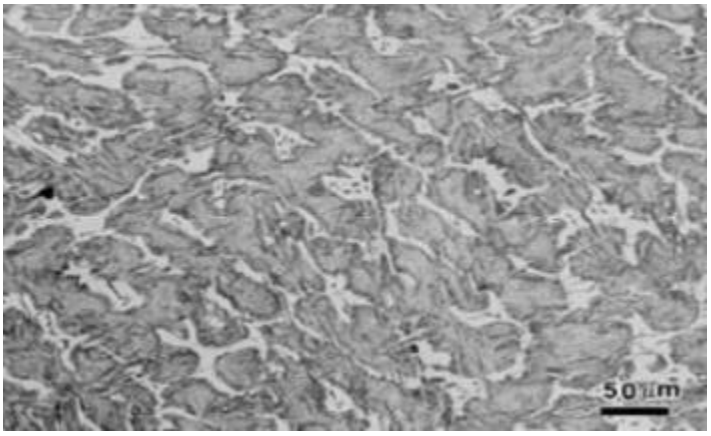

Figure II.5 : Structure cémentite [17].

- **Pearlite**

Pearlite is a combination of ferrite and cementite (α+Fe3C). These two phases are found in alternating layers in the microstructure. Pure pearlite forms at 727°C (1341°F), and contains 0.76% carbon. This phase always contains 0.76% carbon. For steel or cast iron containing more than 0.76% carbon, pearlite is formed with cementite (figure II.6) [17].

Figure II.6 : Structure perlitique [17].

II.4 Conclusion

Steel is an iron alloy containing less than 2% carbon. The types of steels used for the tubes are: low alloy carbon steels, low carbon steels. X70 steel has high ductility and good toughness, which is suitable for pipelines.

the microstructure, hardness, and resilience show that the mechanical properties are suitable for use in the transport of hydrocarbons.

The equilibrium diagram is the most important of all binary alloy systems, it comprises in phases: ferrite, pearlite, cementite.

Referrence:

[1] Pierre HOUSSIN, Georges WESSELS Des matériaux (Jean-Paul Bailon).

[2] laboratoire mécanique Alfa pipe Ghardaïa.

[3] H. Bouhafs, ‘’ Contribution à l’étude des causes de dégradation des conduites du transport d’eau industrielle ‘’, Mémoire de Master, université Badji Mokhtar, Annaba, 2016..

[4] Y. Barkat, ‘’Étude comparative entre deux procédés de soudage des pipelines**,’‘** Mémoire de Master, Université de Biskra ,2016..

[5] A. Debabi, ‘’ Etude des caractéristiques mécaniques d’un joint de soudure après application d’un traitement thermique ‘’, Mémoire de Master, Université Mohamed Boudiaf**,** M’SILA, 2018.

[6] K. Hulka, ‘’HSLA large diameter pipe plate from standard production to X80/X100 ‘’, Niobium Information 13/39, 1997.

[7] ‘’High strength structural and high-strength lowalloy steels ‘’, Metals Handbook**,** Tenth edition, 1990.

[8] Y. Bouguerra et S. Bourahla, ‘’ Analyse structurale de l’acier XC42 du point de vue fissuration à froid en soudage ‘’, Mémoire de Master, Université Mouloud Mammeri, Tizi Ouzou, 2017.

[9] A. Pineau, ‘’Intégrité mécanique des pipelines et gazoducs : enjeux scientifiques et techniques‘’. Séminaire International sur les Technologies Mécaniques : SITEM 09, Tlemcen, 05 et 06 Décembre 2009..

[10] F. Khamouli, ‘’ Influence du flux de soudage sur la qualité de la soudure des Pipelines‘’ , Thèse de Doctorat, Université Badji Mokhtar, Annaba, 2018.

[11] V. Smanio-Renaud, ‘’ Etude des mécanismes de Fragilisation Par l’Hydrogène des aciers non alliés en milieu H2S humide : contribution de l’émission acoustique ‘’, Thèse de Doctorat, l'Institut National des Sciences Appliquées, Lyon, 2008..

[12] Mechanical Metallurgy, G.E. Dieter, chap. 9, The Tension Teste, p. 329-377, Internatl**.** Student Edition McGraw-Hill, 1976.

[13] American Petroleum Institute, (2004), « API Specification 5L » 42nd ed, Washington, D.C, 2004.

Chapter III: Materials studied and experimental techniques

III.1 Introduction

In the first part of this chapter, we present the steel studied and the heat treatment that has been carried out. A second part will then be dedicated to the presentation of the experimental techniques used to characterize this steel.

III.2 Materials studied

The samples studied for this work were taken from a high yield strength grade **API** 5L X70 steel used for oil and gas pipeline transportation, supplied by ALFAPIPE society in Ghardaïa, Algeria. Two types of samples were used, small samples with a size of (10 mm × 10 mm × 9 mm) for metallographic examinations and large samples with a size of (150 mm × 50 mm × 9 mm) for **MBN** measurements. The chemical composition of this steel is given in Table 1 [1].

Table 1: Chemical composition of X70 steel [1]

Elements	C	Mn	S	P	Nb	V	Ti
X70	0.12	1.4	0.03	0.03	0.045	0.048	0.02

III.3 Sample preparation

III.3.1 Heat treatment carried out

The heat treatments that we carried out during this study were made using a NABERTHER type furnace at the **LPM** laboratory of the University of LAGHOUAT Figure (III.1)

Figure III.1: NABERTHERM furnace

III.3.1.1 Treatement direct quenching (DQ) and tempering

- ✓ Heating to inter-critical temperatures. (**ICT**)
- ✓ 30 minutes of holding
- ✓ Water quench (**WQ**) (figure III.2)
- ✓ Tempering at 300 °C, 400 °C and 500 °C

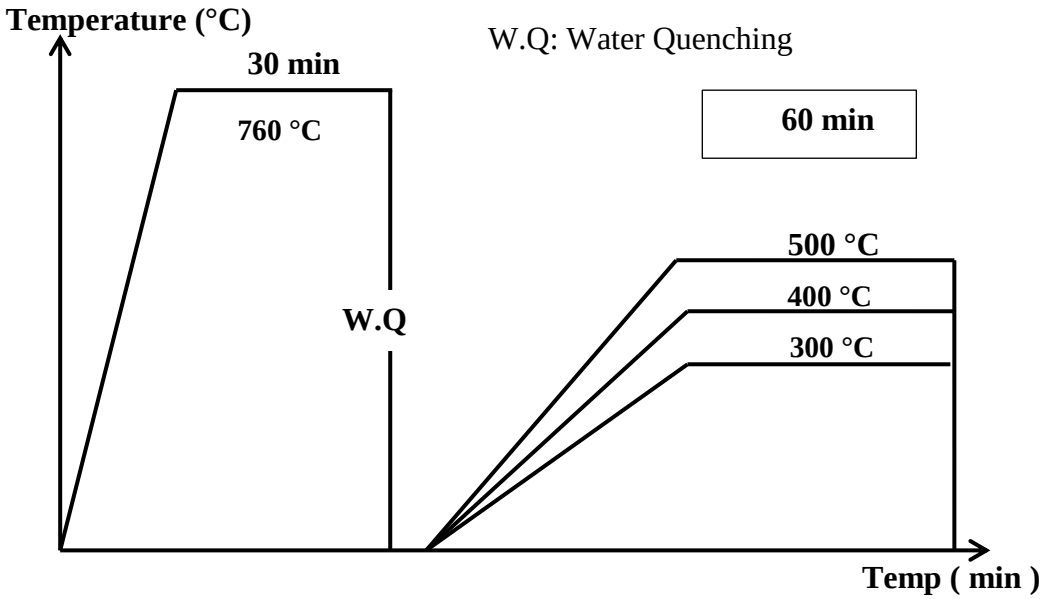

Figure III.2: Schematic illustration of the heat treatment routes

III.3.2 Polishing

A standard protocol was applied to highlight the microstructure of the samples after heat treatment. The samples were polished with water lubrication using a polishing machine, figure (III.3), with different abrasive papers, SiC (silicon carbide). We started polishing with coarse-grained abrasive papers, and will end with fine-grained abrasive papers until the scratches (streaks) disappear. Then we move on to finishing to obtain a mirror surface with a diamond paste or alumina mat.

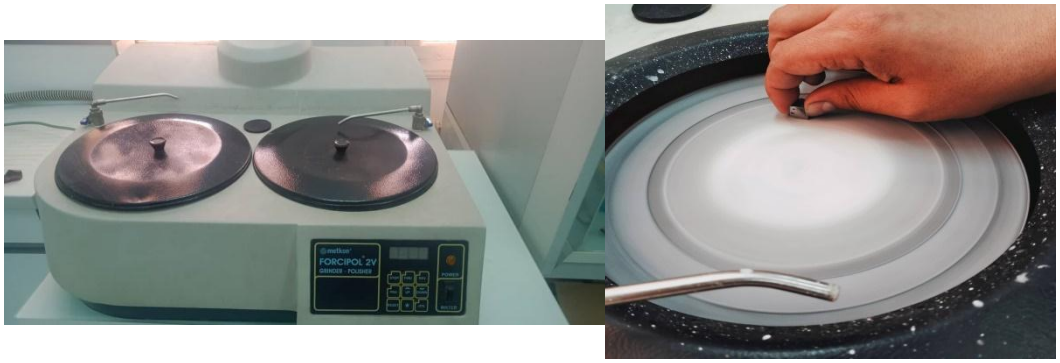

Figure III.3: Polishing machine

III.3.3 Chemical attack

The samples are then etched with a Nital solution (4% nitric acid (HNO3)) and 96 % ethanol (C2H5OH)). The latter is used for examining the grain structures of low alloy and unalloyed steels. The mirror surface obtained by polishing is immersed in Nital for about 10 to 15 seconds in order to reveal the microstructure, and this is manifested by the disappearance of the mirror state (matte). Then the sample must be rinsed with water to stop the effect of the chemical attack.

Figure III.4: Chemical attack

III.4 Metallographic examination

After a final cleaning, the samples are ready for observation under an optical microscope (**OM**) or the **SEM** (Scanning Electron Microscope).

III.4.1 Optical microscopy

The samples are then observed under optical microscopy. Optical microscopy of the LIECA DMLM type with different magnifications at the level of the process engineering laboratory at the mechanical engineering department of the university of LAGHOUAT figure, (III.5).

Figure III.5: Optical microscopy

III.5 Hardness measurements H_V

The device used is a universal rebound hardness tester (Hardness Testing System Model: Th180). We perform several Vickers hardness measurements $\mathbf{H_V}$ on each sample in order to obtain an average value representative of the overall Vickers hardness.

III.6 Experemental

The specimens, 9 mm thick, were prepared from a high yield strength grade API 5L X70 steel. All specimens were quenched in water after heating at an inter-critical temperature (Direct quenching treatment) at 760 °C for 30 minutes. Then, specimens were separately tempered at 300°C, 400°C and 500°C for 60 minutes.

Before metallographic investigation, the samples were polished with silicon carbide paper, then etched with 4% Nital to obtain a mirrored surface. The microstructure examinations were done using an optical microscope. An average hardness value was determined by measuring Vickers hardness at different locations.

MBN measurements were performed using a **MikroMach** system. A sinusoidal cyclic magnetic field with an excitation frequency of 40Hz was induced in a small volume. The BARKHAUZEN signals were filtered with a wide high-pass filter (2–24 kHz), amplified, and then analyzed using the **MMS** software.

III.6.1 Results and Discussions

III.6.1.1 Microstructure and Hardness

Representative micrographs (Figure 2) and hardness values (Table 2) of the samples show that typical ferrite-martensite structure (Fig.2 a). Ferrite remains essentially unchanged, and the perlite decomposes into carbon-rich austenite. As long as the martensite transforms without diffusion, it inherits the quantity of carbon from the austenite fixed by the IAT. In the ($\alpha + \gamma$) domain, the first structure (ferrite + perlite) is reheated; the austenite grows within the perlite regions. At this time, austenite germinates on the boundaries of ferrite grains. After quenching with water, this austenite is transformed into islands of martensite [1]. tempered structures (Fig.2 b-d) were successfully obtained.

Figure 2. shows a microstructure obtained by optical microscopy of specimens that underwent inter-critical annealing at 760 °C followed by tempering at 300 °C, 400 °C and 500 °C. The microstructure consists of a ferrite matrix (F) and islands of hard martensite (M). During the process, the carbides (C) can be observed in the microstructure. The increase of the tempering temperature induces carbide precipitation which leads to an increase of its size.

The ferrite is covered with numerous carbide particles when the tempering temperature reaches 300 °C. This is in accordance with what is reported in the literature as several researches [**2**], assert that the carbides start to precipitate inside the ferrite grain when the tempering temperature is increased to about 300 °C [**3**].

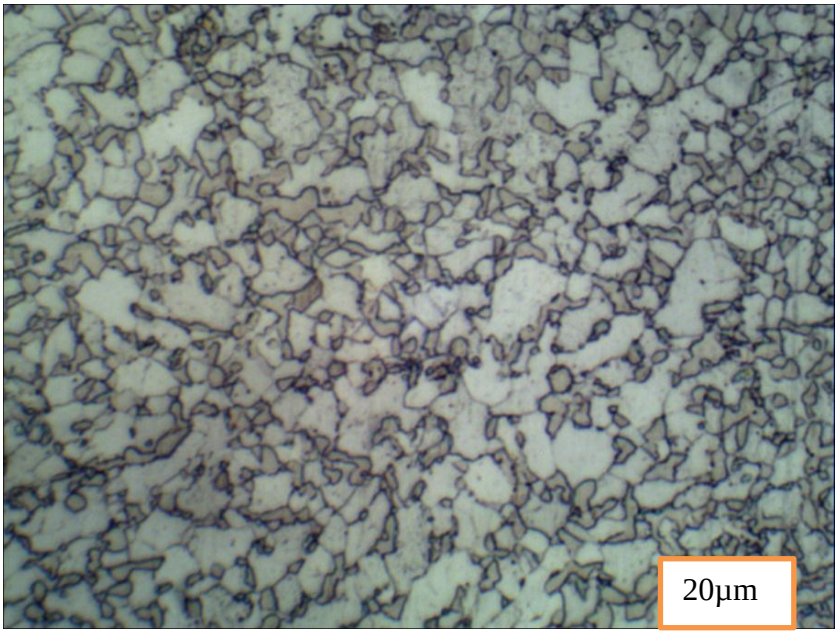

a- As- quenched 760 °C

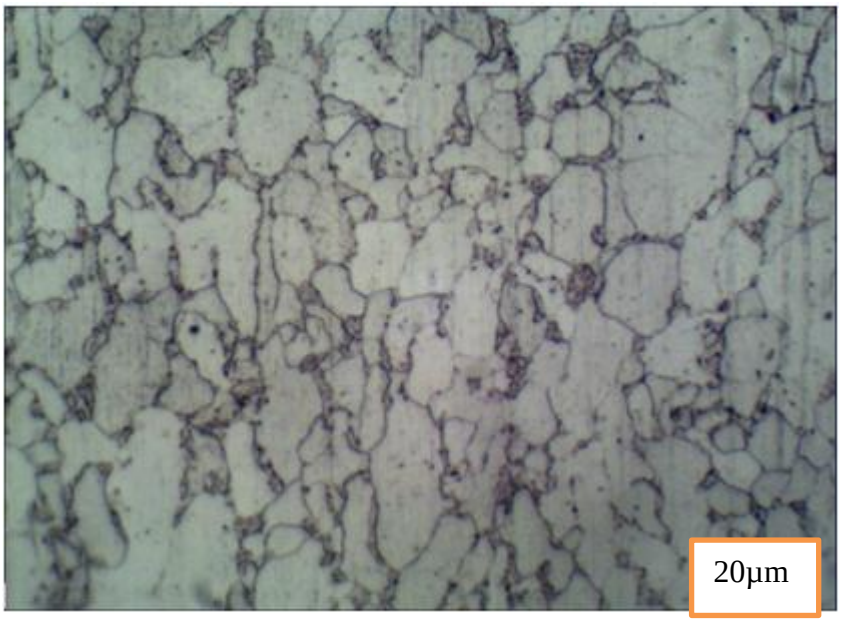

b- Tempered at 300 °C

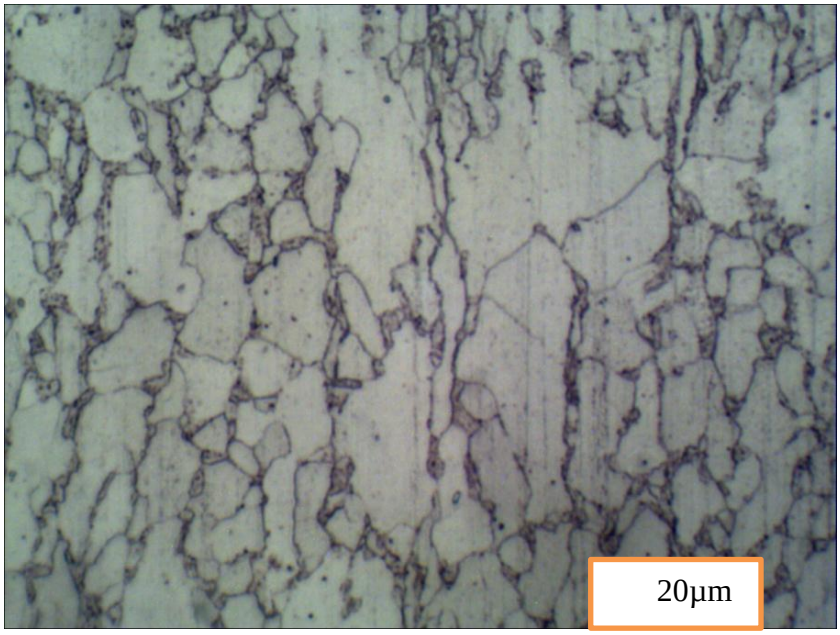

c- Tempered at 400 °C

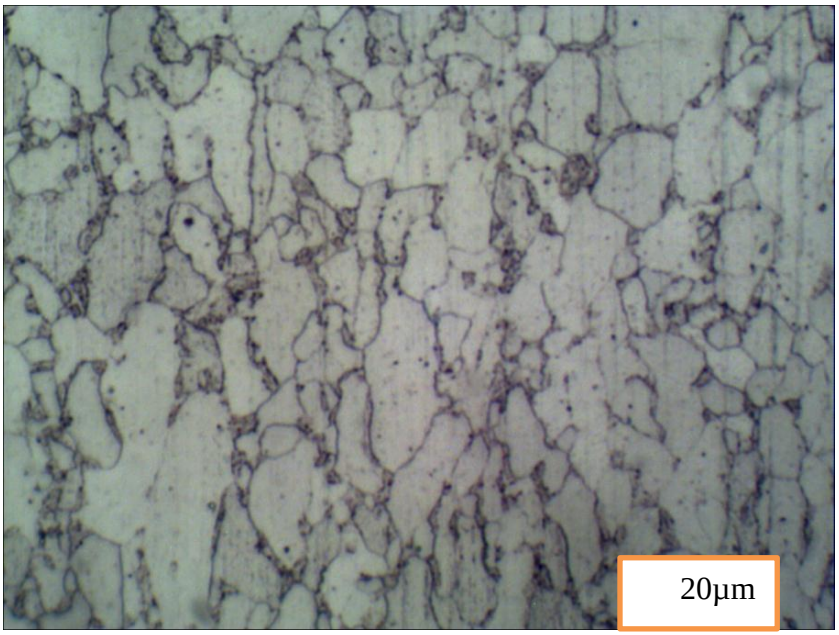

d- Tempered at 500 °C

Figure 2. Representative Micrographs of the Samples

Table 2 – Hardness Values and MBN Parameters of the Specimens

Specimen	Hardness [HV]	Mmax (mV)	Hcm (A/cm)
As-quenched	220	0.33	17.79
300 °C- tempered	195	0.37	17.69
400 °C- tempered	193	0.39	13.27
500 °C- tempered	184	0.42	4.32

III.6.2 BARKHAUSEN Noise

The results show that magnetic BARKHAUSEN noise is influenced by the tempering which, as a function of the temperature, causes changes in dislocation density, lattice straining (i.e., micro residual stresses) and the morphology and size of ferrite and martensite, and corresponding variations in hardness.

Under the effect of an alternating magnetic field, a representative magnetic hysteresis loop was induced in the small volume measured due to the energy loss with the irreversible process of magnetization. This irreversible process is strongly related to the dynamic behavior of domains, i.e., nucleation, annihilation and growth of domains. Grain/lathe boundaries, dislocations and precipitates affect this dynamic behavior. Consequently, the number of domain walls moving at a given instant and the mean free path of the domain wall displacement decide the MBN peak height [2].

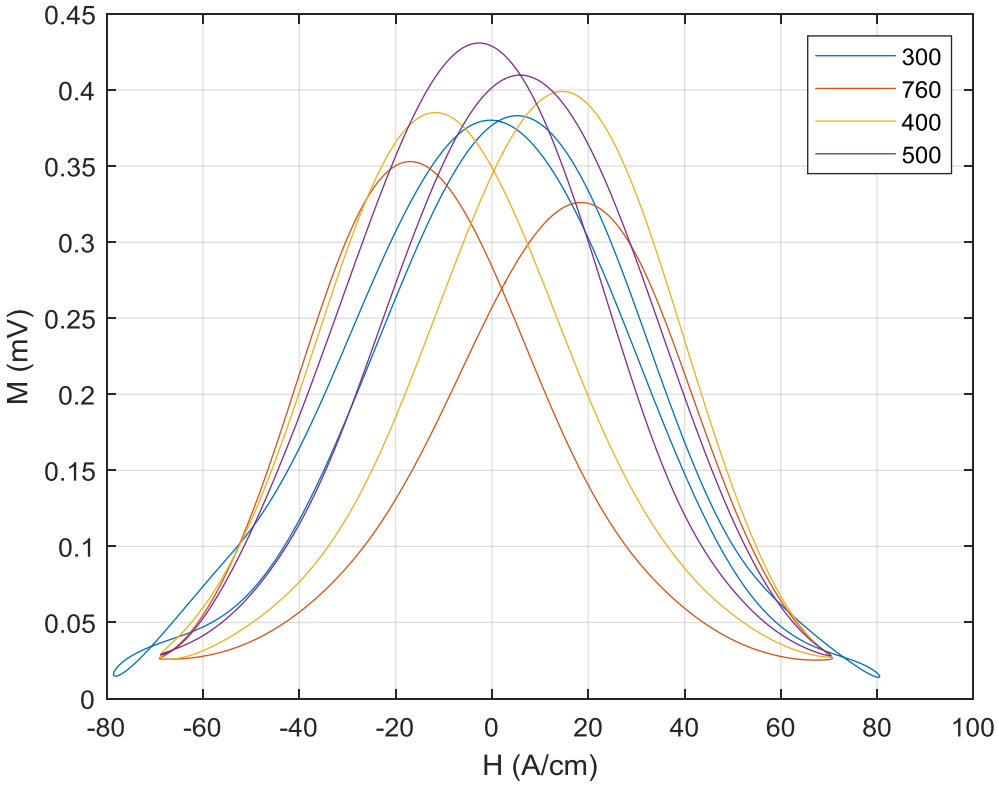

Figure 3. MBN of the Samples

Figure 3 shows the graph for MBN signal versus applied field strength. The as-quenched sample has the weakest MBN peak positioned at the highest field linked with the high coercivity of fettite-martensite. Tempering up to 300 °C slightly increases the peak height whereas tempering at 400 °C and 500 °C increases peak height drastically. Moreover, the coercive field of the signal shifts to the lower values of magnetic field due to tempering. As the tempering temperature increases, the low amplitude broad peak of as-quenched transforms into a high amplitude peak situated at low magnetic field.

In the as-quenched specimen, the body-centered consists of a ferrite matrix (F) and an island of hard martensite (M) determines the domain structure. Since the magnetic structure consists of very small domains due to small islands, relative volume occupied by a domain wall is larger.

Besides, high dislocation density in the ferrite and martensite laths acts as a barrier to the movement of domain walls. A strong field is required for the reversal of magnetization because of low domain wall displacements and difficulty in nucleating domain walls. Presence of micro residual stresses in the martensite islands has an additional effect on reduction of the MBN response.

Tempering at 300 °C changes the microstructure very slightly. Although ε-carbides form, the microstructure is still islands shaped. Therefore, the height and position of the MBN peak do not change significantly. During tempering at 400 °C and 500 °C, temperature induces carbide precipitation which leads to an increase of its size [2].

III.6.3 Hardness Correlation

The raw data consists of a series of voltage pulses and associated magnetic field values. The response of RMS of the noise signals over several field cycles to the changes in microstructure is similar to that of MBN peak height. It is seen in Fig.2 that the as-quenched specimen (the hardest one) has the lowest RMS value. As tempering temperature increases, in contrast to the decrease in hardness, RMS value decreases. Pinned domain walls due to high dislocation density and small ferrite and martensite islands cause lower RMS values. As tempering temperature increases dislocation density decreases, micro residual stresses diminish and the magnetic structure comes close to those of a ferrite. Thus, RMS value decreases.

Figure 4 shows the correlation graph between the Mmax and Hc values of the MBN signal with the hardness of specimens. We can see an excellent correlation between the MBN values with hardness.

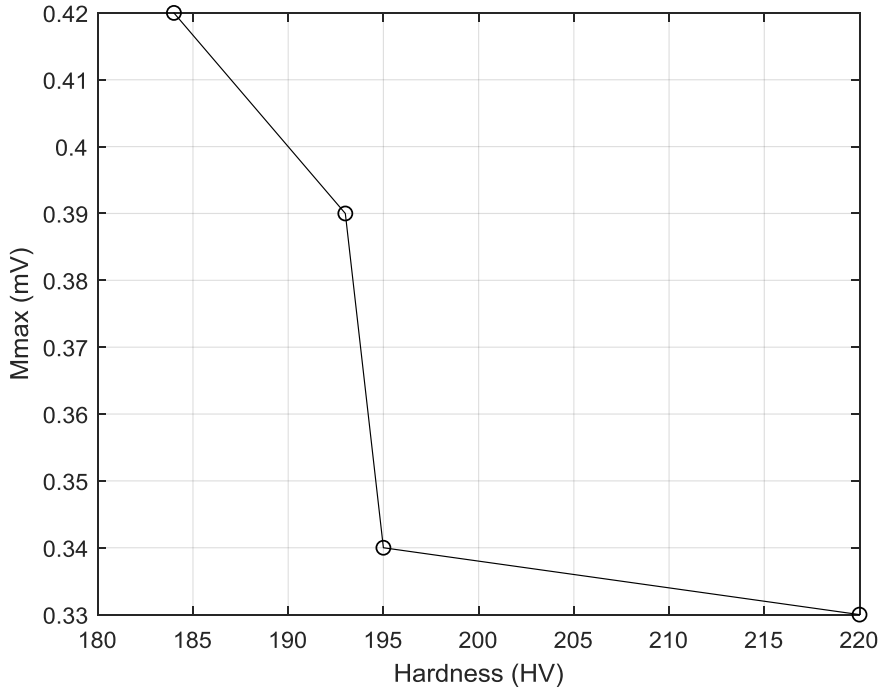

Figure 3. Correlation between Mmax and Hardness.

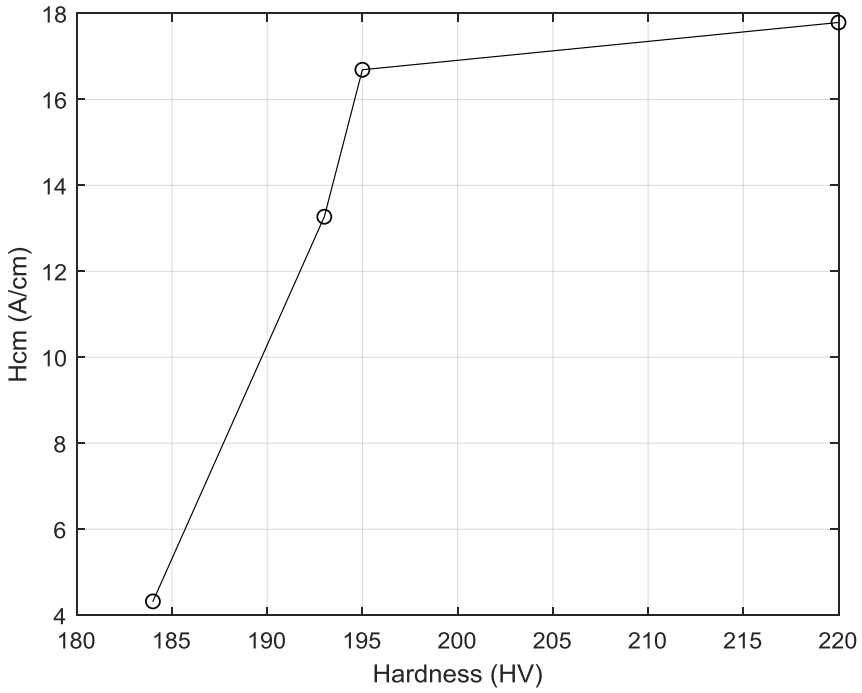

Figure 4. Correlation between Hcm and Hardness.

III.6.4 Conclusions

Microstructures of the quenched and tempered X70 steel specimens were characterized by Magnetic BARKHAUZEN Noise measurements. MBN method is a powerful tool for evaluating different stages of tempering. In the as-quenched sample, pinned domain walls due to high dislocation density and small martensite islands cause low MBN activity; and MBN peak is at higher magnetic fields due to small domain wall displacements and difficulty in domain nucleation. All in all, an excellent correlation exists between the Mmax and Hc values and hardness. Finally, this method can be utilized efficiently and effectively for evaluating the hardness and the microstructure of the steel components.

Reference:

[1] Hocine Nebair, 1 August 2022.

[2] S. Gunduz: Mater Lett, 63 (2009) 2381-2383.

[**3**] H. Li, S. Gao, Y. Tian, D. Terada, A. Shibata, N. Tsuji: Mater Taday Proc, 2 (2015) S667 S671.

General conclusion

In this work, we measured the magnetic characteristics of a few ferromagnetic materials, in this instance alloy steels X70, used for the transportation of hydrocarbon.

A bibliographic research on the BARKHAUSEN noise technique and magnetic phenomena was carried out.

The data collected demonstrate that BARKHAUSEN noise measurements can reveal information about a material's crystalline microstructure, magnetic microstructure, and mechanical and magnetic hardness.

DQ treatment revaled a microstructure consisting of hard martensite distributed in the ductill ferrite matrix.

We fined a direct correlation between magnetic hardness Hc and mechanical hardness Hv for DQ treatment.

الملخص:

الهدف من هذا العمل هو دراسة ابنية الدقيقة للفولاذ المسقي والمقاوم بطريقة لا تجعله يفقد خصائصه بواسطة تقنية الضوضاء BARKHAUZEN المغناطيسية. تم تحضير نوعين من العينات من القضبان الفولاذية X70. تم تسخين جميع العينات عن طريق التبريد المباشر (DQ) عند **760** درجة مئوية لمدة 0.5 ساعة. تم بعد ذلك تلطيف العينات المروية عند درجات حرارة مختلفة بين 300 درجة مئوية و **400** درجة مئوية و 500 درجة مئوية. تم توضيح تكوين الهياكل المجهرية المرغوبة من خلال فحوصات المعادن وقياسات الصلابة. في جميع العينات تم وصف موضع وشكل وسعة إشارات BARKHAUZEN باستخدام نظام MikroMach.

الكلمات المفتاحية: السقي، التلطيف، باركهاوزن، البنية المجهرية، المعالجة الحرارية.

Abstract:

The aim of this work is to study the microstructures of quenched and tempered steels non-destructively using the Magnetic BARKHAUZEN Noise technique. Two types of samples were prepared from X70 steel bars. All samples were heated by direct quenching (DQ) at 760 °C for 0.5 hours. The quenched samples were then tempered at various temperatures between 300°C , 400°C and 500°C. Formation of the desired microstructures was demonstrated by metallographic examinations and hardness measurements. In all specimens, the position, shape, and amplitude of the BARKHAUZEN signals were described using a MikroMach system.

Key words: Quench,Temper, BARKHAUZEN, microstructures, metallographic,temperature treatement.